



Does maximization of net carbon profit enable the prediction of vegetation behaviour in savanna sites along a precipitation gradient?

Remko C. Nijzink¹, Jason Beringer², Lindsay B. Hutley³, and Stanislaus J. Schymanski¹

¹Luxembourg Institute of Science and Technology

²University of Western Australia, Crawley, Australia

³Charles Darwin University, Darwin, NT, Australia

Correspondence: R.C. Nijzink (remko.nijzink@list.lu)

Abstract.

Most terrestrial biosphere models (TBMs) rely on more or less detailed information about the properties of the local vegetation. In contrast, optimality-based models require much less information about the local vegetation as they are designed to predict vegetation properties based on general principles related to natural selection and physiological limits. Although such models are not expected to reproduce current vegetation behaviour as closely as models that use local information, they promise to predict the behaviour of natural vegetation under future conditions, including the effects of physiological plasticity and shifts of species composition, which are difficult to capture by extrapolation of past observations.

A previous model intercomparison using conventional terrestrial biosphere models revealed a range of deficiencies in reproducing water and carbon fluxes for savanna sites along a strong precipitation gradient of the North Australian Tropical Transect (Whitley et al., 2016). Here we examine the ability of an optimality-based model (the Vegetation Optimality Model, VOM) predict vegetation behaviour for the same savanna sites. The VOM optimizes key vegetation properties such as foliage cover, rooting depth and water use parameters in order to maximize the Net Carbon Profit (NCP), defined here as the difference between total carbon taken up by photosynthesis minus the carbon invested in construction and maintenance of plant organs.

Despite a reduced need for input data, the VOM performed similarly or better than the conventional TBMs in terms of reproducing the seasonal amplitude and mean annual fluxes recorded by flux towers at the different sites. It had a relative error of 0.08 for the seasonal amplitude in ET, and was among the best three models tested with the smallest relative error in the seasonal amplitude of gross primary productivity (GPP). Nevertheless, the VOM displayed some persistent deviations from observations, especially for GPP, namely an underestimation of dry season evapo-transpiration at the wettest site, suggesting that the hydrological assumptions (free drainage) have a strong influence on the results. Furthermore, our study exposes a persistent overprediction of vegetation cover and carbon uptake during the wet seasons by the VOM. Our analysis revealed several areas for improvement in the VOM, including a better representation of the hydrological settings, as well as the costs and benefits related to plant water transport and light capture by the canopy.

The results of this study imply that vegetation optimality is a promising approach to explain vegetation dynamics and the resulting fluxes. It provides a way to derive vegetation properties independently from observations, and allows for a more insightful evaluation of model shortcomings as no calibration or site-specific information is required.



1 Introduction

Current state-of-the-art terrestrial biosphere models (TBMs) commonly rely on locally observed vegetation properties and/or phenology (e.g. species composition, leaf area index dynamics) and informed guesses where observations to calibrate parameters are not available (e.g. rooting depths) (Whitley et al., 2016). At the same time, many model parameters are assumed to be invariant in time and space, such as prescribed rooting depth, which does not adapt to seasonal and longer-term changes in environmental conditions. As a result, TBMs often struggle to reproduce the dynamics of observed carbon and water fluxes, notably in seasonal environments such as savanna ecosystems, and are often outperformed even by simple regression models (Best et al., 2015; Whitley et al., 2016). Furthermore, calibration of vegetation properties on past observations may limit the utility of the models for predictions in a changing environment (Schulz et al., 2001) or outside the environment used to develop and/or parameterize them. Therefore, novel methods to capture the dynamic adaptation of vegetation-related parameters in terrestrial biosphere models are urgently required given changing climates and disturbance regimes (Schulz et al., 2001; Whitley et al., 2016).

Following Whitley et al. (2016), we include in the definition of TBMs land surface models, dynamic global vegetation models and stand-scale models. The boundaries between these different model types are slowly disappearing as most models attempt to capture both the vegetation and hydrological processes in order to improve their original purpose of simulating energy exchange (Prentice et al., 2015). TBMs that require site-specific vegetation properties, for example, but not limited to, leaf area index or rooting depths, including widely used models such as the Soil, Plant, Atmosphere model (SPA Williams et al., 1996a) and BESS (Ryu et al., 2011, 2012), often produce satisfactory results, but they strongly depend on the quality of the prescribed vegetation data. Therefore, these models are of limited utility for modelling responses to changing environmental conditions, which is particularly important for longer-term predictions.

Model intercomparison studies have revealed several persistent deficiencies of terrestrial biosphere and land surface models. In the past, Pitman et al. (1999) noted already that 16 land surface models strongly deviated from observations especially at the seasonal time scale and in relation to evaporation, and thus vegetation. Also later, Pitman et al. (2009) did not find consistent responses to land cover change by seven climate models, which was explained by strongly differing ways to model evapotranspiration and phenology. More recently, Teckentrup et al. (2021) evaluated 13 dynamic global vegetation models for Australia which simulated widely differing magnitudes of net biome productivity for the continent at decadal to centennial time scales. Differences in model performance were attributed to a variety of simulated carbon residence times and, at centennial time scale, simulated responses to land use change. Best et al. (2015) showed that the sensible heat flux was strongly overestimated by a set of 13 land surface models, which could also be explained by an underestimation of the latent heat flux, because of the misrepresentation of vegetation in the model. The importance of vegetation was highlighted by Whitley et al. (2016), who showed that deviations between modelled and observed data could be partly explained by incorrect assumptions about rooting depths and the use of static phenology for the highly dynamic savanna vegetation. Along similar lines, Dirmeyer (2011) argued that improvements of land surface models should focus on including the carbon cycle through plants and bacteria, but also, for example, phenology, plant respiration and carbon pools.



60 So far, only a small number of models simulate vegetation dynamics in a prognostic way. For example, LPJ-GUESS (Smith et al., 2001) simulates growth and competition between five different plant functional types with prescribed, static properties for each. Other models, such as Tethys-Chloris (Fatichi et al., 2012) or RHESSys (Tague, 2004), use allocation schemes for carbon, but use prescribed and static vegetation partitions for different plant functional types or species.

In order to improve the generality of TBMs, the implementation of organizing principles, such as optimality, has been
65 proposed by an increasing number of scientists (e.g. Eagleson, 1982; Rodríguez-Iturbe and Rinaldo, 2001; McDonnell et al., 2007; Schymanski et al., 2007; Franklin et al., 2012; Bonan et al., 2014; De Kauwe et al., 2015; Haverd et al., 2016; Buckley et al., 2017; Wang et al., 2017, 2018; Franklin et al., 2020). Optimality assumes that a system self-optimizes in order to maximize or minimize some goal function related to plant survival (e.g. maximum productivity or minimum stress) or self-maintenance of system compartments, such as entropy production or power extraction (Schymanski et al., 2009a). This means
70 that system properties and behaviour with trade-offs related to said goal function can be predicted rather than prescribed based on past observations or calibration.

Following this paradigm, Schymanski et al. (2007, 2009b) proposed that vegetation may self-optimize to maximize its Net Carbon Profit (NCP) and identified costs and benefits of various vegetation properties with respect to NCP. Schymanski et al. (2015) applied this principle to simulate effects of elevated atmospheric CO₂-concentrations on vegetation across several sites
75 in Australia and found that the results were consistent with experimental evidence. In a similar study, Wang et al. (2018) found that the inclusion of the maximum NCP optimality principle to model optimal root systems improved the simulation of water use by phreatophytic vegetation in the widely used land surface model NOAH-MP. In contrast to these successful applications of optimality, Dekker et al. (2010) reported a 38% overestimation of CO₂-assimilation, when applying the maximum NCP principle in a Douglas fir plantation in the Netherlands. It is not clear if this bias was due to invalidity of the maximum NCP
80 principle, missing model constraints, the short duration over which the optimization was performed (1 year) or the limitations to optimal adaptation by the choice of species and plantation tree density. More thorough testing of the validity of the maximum NCP principle is therefore needed, especially in natural vegetation, which is in a near-equilibrium, optimal state with its environment.

These natural conditions can be found in savanna ecosystems, that can broadly be defined as a co-existence of trees and
85 grasses and have evolved over millions of years in highly specialized, extremely seasonal environments (Beerling and Osborne, 2006; Rowe et al., 2020). At present, savannas contribute up to 30% of the global net primary productivity (Grace et al., 2006; Lehmann et al., 2014) and understanding their behaviour is crucial for predicting the effects of global change. At a global-scale, the distribution of savannas are tightly coupled to the occurrence of wet-dry seasonal climates, namely the savanna climate type as defined by Köppen-Geiger (Peel et al., 2007; Beck et al., 2018). These ecosystems are highly dynamic due to the seasonality
90 of the climate which in turn drives dramatic changes in phenology and productivity of both woody and grassy components (Scholes and Archer, 1997; House et al., 2003). In north Australian savannas, the properties of overstorey trees, such as the height, relate to the rainfall amount and soil type (Williams et al., 1996b), whereas tree water use remains rather stable over the seasons (O'Grady et al., 1999; Hutley et al., 2000; Kelley et al., 2007). The combination of co-occurring seasonal grasses, relatively deep-rooting perennial trees, frequent fire and strong re-sprouting capacity in savannas presents a set of challenges for



95 vegetation models, which struggle to reproduce variation in soil water and vegetative cover, particularly between overstorey
and understorey vegetation (Baudena et al., 2015). For these reasons, the savanna sites along the North Australian Tropical
Transect (NATT) provide an excellent living laboratory (Hutley et al., 2011), especially as the strong rainfall gradient from
north to south (approx. 1 mm mean annual rainfall per km south) provides different climatological circumstances, whereas
other factors as topography and soils remain rather constant. Moreover, moisture availability is known to be one of the main
100 drivers of vegetation behaviour in savannas (Scholes and Archer, 1997), which makes the transect well-suited for studies on
the effect of precipitation on vegetation (Hutley et al., 2011), either observation based (Ma et al., 2013; Moore et al., 2016) or
model based (Haverd et al., 2013; Whitley et al., 2016).

The savanna sites of the NATT used in the model intercomparison study by Whitley et al. (2016) revealed a range of
deficiencies in the TBMs used. Most of the models required information about vegetation cover as an input, whereas only one
105 of the models (LPJ-GUESS) represented vegetation in a dynamic way. This reflects also the wider spectrum of TBMs, as few
models predict vegetation dynamics, and the few that do, rely on prescribed behaviour of a few plant functional types deemed
representative for a given site. In addition, as Whitley et al. (2016) pointed out, the interplay between shallow rooted (0.5-1.0
m) seasonal vegetation and deep-rooted (>2.0 m) perennial vegetation is an important factor controlling fluxes in savannas.
This relates to the strong seasonality in water availability in these ecosystems, which leads to issues for models that prescribe
110 constant rooting depths of around 2.0 m or less. Finally, Whitley et al. (2016) showed the importance of disturbances, most
notably fires, in shaping the community composition, structure and fluxes in savannas (Scheiter et al., 2013), but the models in
their study did not consider such disturbances. So far, there are only a few models that explicitly model savanna-like fire events,
such as aDGVM (Scheiter and Higgins, 2009). This model has been used to model spatial and temporal patterns of biomass
accumulation in both African (Scheiter and Higgins, 2009) and Australian savannas (Scheiter et al., 2015) and demonstrated
115 how fire management practices and climate change may influence carbon uptake and storage in savanna vegetation.

The above-mentioned studies all indicate the need for improvements in TBM applications that are able to explicitly model
vegetation dynamics in the first place. The Vegetation Optimality Model (VOM, Schymanski et al., 2009b, 2015) explicitly
models vegetation dynamics by optimizing vegetation properties for the NCP. The VOM quantifies carbon costs for the main-
tenance of leaf area, photosynthetic capacity and root surface area based on empirical studies, as described in Schymanski
120 et al. (2007, 2008), that allows for a systematic and consistent explanation of vegetation behaviour under different external
conditions at different sites. So far, the VOM has been applied successfully by Schymanski et al. (2009b) and Schymanski
et al. (2015), but these previous applications exhibited several shortcomings as well. For example, the carbon cost parameter
for water transport tissues could not be estimated based on literature and was instead calibrated by (Schymanski et al., 2009b)
at a relatively wet savanna site, the Howard Springs eddy covariance site (Fluxnet code AU-How, Beringer et al., 2016). This
125 calibration aimed at reproducing the dry season vegetation cover, and led to a calibrated value within a relatively narrow range
of +0.1 and -0.1 $\mu\text{mol m}^{-3} \text{s}^{-1}$ (i.e. a range of 0.2 $\mu\text{mol m}^{-3} \text{s}^{-1}$). However, the efficiency of plant hydraulics can depend on
environmental conditions such as temperature or water stress (Roderick and Berry, 2001; Mencuccini et al., 2007; Hacke et al.,
2001), indicating that the carbon cost related to the water transport system, that facilitates the plant hydraulics, may depend on
these conditions as well. At the same time, the VOM-application by Schymanski et al. (2009b) predicted a vegetation cover



130 of 100 % at Howard Springs, in contrast with remotely sensed observations. This was explained by a low-bias in the remotely
sensed vegetation due to seasonal lagoons within the grid cell, but applications of the VOM under a wider range of environ-
mental conditions should provide a more thorough evaluation of the correctness of the predicted vegetation cover. In general,
a systematic evaluation of the prognostic vegetation properties under different climatological conditions is still missing, also
in comparison with traditional modelling approaches. For example, most of the models in the large model intercomparison
135 study of Whitley et al. (2016) prescribed vegetation cover based on leaf area index observations, and assumed constant rooting
depths. However, rooting depths are known to strongly vary with precipitation Schenk and Jackson (2002), but is likely to
change over the precipitation gradient of the NATT (Williams et al., 1996b).

For these reasons, we apply the VOM to the same savanna sites that were used in the model intercomparison by Whitley et al.
(2016) along the North Australian Tropical Transect (NATT, Hutley et al., 2011). Using this experimental framework, we could
140 test the VOM and the vegetation optimality principles, over a well-defined environmental gradient, and a comparison could be
made with several state-of-the-art TBMs that were used by Whitley et al. (2016). We formulated the following hypotheses:

1. The optimality-based model is not substantially worse at capturing the seasonal amplitudes and mean annual values of
observed carbon and water fluxes than conventional models analyzed by Whitley et al. (2016) along the NATT.
2. Re-calibration of the water transport cost parameter to reproduce remotely sensed dry season vegetation cover at each
145 site will not result in large variation (more than $0.2 \mu\text{mol m}^{-3} \text{s}^{-1}$) of this parameter between sites.
3. Replacing predicted vegetation cover in the VOM by remotely sensed vegetation cover does not lead to a better repro-
duction of observed seasonal amplitudes and mean annual fluxes.
4. Using a prescribed, homogeneous rooting depth in the VOM instead of prognostic rooting depths leads to a worse
reproduction of observed seasonal amplitudes and mean annual fluxes.

150 2 Methodology

The hypotheses were addressed by setting up the VOM for five study sites along the North Australian Tropical Transect and
several numerical experiments were defined, as described respectively in Sect. 2.1 and 2.3. More details about the VOM and the
long-term and short-term optimization of the Net Carbon Profit can be found in 2.2. All the data pre- and post-processing and
model runs were done in an open science approach using the RENKU¹ platform as a tool to make the research reproducible,
155 enable transparent numerical analyses, and track all steps in the scientific process. The entire workflow including code and
input data can be found online².

¹<https://renkulab.io/>

²<https://renkulab.io/gitlab/remko.nijzink/vomcases>



2.1 Study sites

In order to test the VOM across a precipitation gradient and compare to the modelling outputs of Whitley et al. (2016), the same study sites of the North Australian Tropical Transect (NATT, Hutley et al., 2011) were selected. These savanna sites are located between $12.5^{\circ}S$ and $22.5^{\circ}S$ that spans a distance of approximately 1000 km (Figure 1 and Table 1) and mean annual precipitation increasing from the most southern sites towards the north from 500 to 1700 mm/year (Figure 1).

The wettest and most northern site of the NATT is Howard Springs (How-AU), with an average precipitation of 1747 mm/year (SILO Data Drill, Jeffrey et al., 2001, calculated for 1980-2017). This study site is an open-forest savanna site, with mostly evergreen overstorey (mainly *Eucalyptus miniata* and *Eucalyptus tetradonta*) and an understorey dominated by annual *Sorghum* and *Heteropogon* grasses. Soils are well-drained red and grey kandosols, with a high gravel content and a sandy loam structure. The flux tower at this site provides the longest record of carbon dioxide and water fluxes along the NATT, starting in 2001 (Beringer et al., 2016).

Adelaide River (AU-Ade) is geographically close to Howard Springs, but has a significantly lower mean annual precipitation of 1497 mm/year (SILO Data Drill, Jeffrey et al., 2001, calculated for 1980-2017). The overstorey is dominated by *Eucalyptus tectifica*, *Corymbia latifolia* and *Planchonia careya*, while the understorey is composed of annual *Sorghum* and *Chrysopogon fallax* grasses. Here, soils are less well-drained and consist of yellow hydrosols with a silt loam and sandy clay loam structure. The fluxes were measured at this site from 2007 until 2009.

Further along the precipitation gradient, we chose the Daly River site (AU-Das) for this study with an average rainfall of 1166 mm/year (SILO Data Drill, Jeffrey et al., 2001, calculated for 1980-2017). Given the reduced rainfall, the Daly River site has a slightly different species composition in the overstorey, with *Terminalia grandiflora*, *Eucalyptus tetradonta* and *Corymbia latifolia* dominating. The soils are deep well-drained red kandosols with a sandy loam structure. The flux tower at Daly River provides data from 2007.

The Dry River site (AU-Dry) is 165 km further south along the transect and is representative of a woodland savanna with a mean annual precipitation of 898 mm/year (SILO Data Drill, Jeffrey et al., 2001, calculated for 1980-2017). Again, an open canopy structure dominated by *Eucalyptus tetradonta* and *Corymbia latifolia* is present with a *Sorghum* and *Heteropogon triticeus* understorey. Soils are again well-drained sandy loam red and grey kandosols with a high gravel content. Here, observations of fluxes are available from 2008.

The most southern and driest site is Sturt Plains, that is not a savanna site, but a natural Mitchell grassland dominated by *Astrabla* grasses (Hutley et al., 2011) and no perennial overstorey species. These are extensive ecosystems throughout the semi-arid regions of northern Australia and occupy the 400-650 mm rainfall zone. The mean annual rainfall at Sturt Plains is 616 mm/year (SILO Data Drill, Jeffrey et al., 2001, calculated for 1980-2017). The contrasting vegetation is due to the soil type that is a defining characteristic of this ecosystem, being a cracking gray vertisol with a silty clay texture. Flux tower measurements at this site start from 2008. Hutley et al. (2011) and Table 1 provide more details on the study sites.

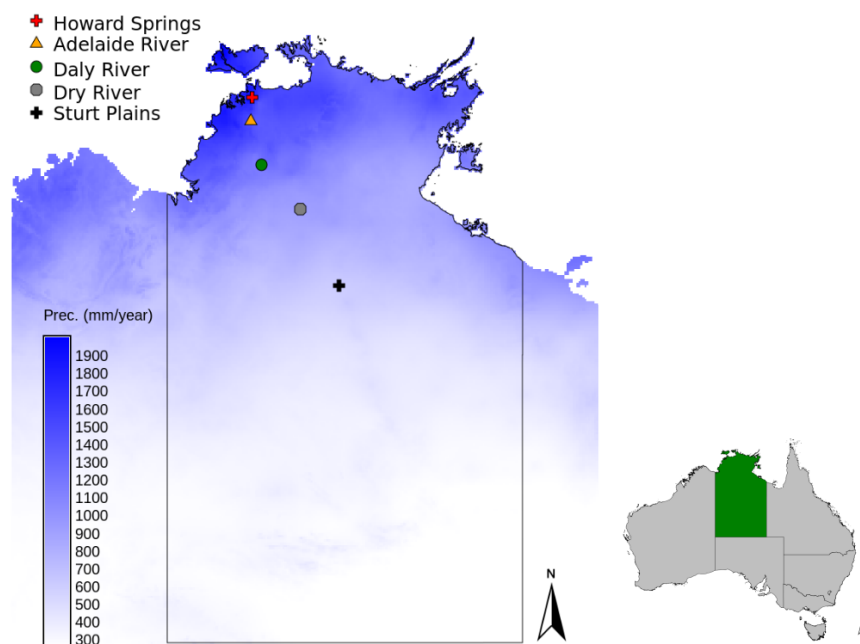


Figure 1. Locations of the study sites along the North Australian Tropical Transect in the Northern Territory of Australia, with the mean annual precipitation shown in the blue colorscale (SILO Data Drill, Jeffrey et al., 2001, calculated for 1980-2017).

2.2 Vegetation Optimality Model

190 The Vegetation Optimality Model (VOM, Schymanski et al., 2009b, 2015) couples a vegetation and water balance model and optimizes vegetation properties in order to maximize the Net Carbon Profit. The model code and documentation can be found online³⁴ and version v0.5⁵ of the model was used in this study. The model is described in more detail in Schymanski et al. (2009b, 2015) and more specifics about the current model set-up can be found in the accompanying technical note Nijzink et al. (2021). For completeness, a brief description of the model is given below.

195 2.2.1 Vegetation model

The VOM represents seasonal grass vegetation and perennial trees by two big leaves in the model. The VOM optimizes photosynthetic capacity, projected foliage cover and stomatal conductance dynamically in order to, eventually, maximize the overall Net Carbon Profit (NCP) for the entire simulation period. The carbon cost of photosynthetic capacity is defined by maintenance respiration, projected cover to the turnover and maintenance of leaf area, while stomatal conductance is linked to

³<https://github.com/schymans/VOM>

⁴<https://vom.readthedocs.io>

⁵<https://doi.org/10.5281/zenodo.3630081>



Table 1. Characteristics of the study sites along the North Australian Tropical Transect, vegetation data from Hutley et al. (2011), Hutley (2015) and Whitley et al. (2016), with Eucalyptus (Eu.), Erythrophleum (Er.), Terminalia (Te.), Corymbia (Co.), Planchonia (Pl.), Themeda (Th.), Heteropogon (He.), and Chrysopogon (Ch.). Meteorological data is taken from the SILO Data Drill (Jeffrey et al., 2001) for the model periods of 1-1-1980 until 31-12-2017, with the potential evaporation calculated according to the FAO Penman-Monteith formula (Allen et al., 1998). The ratio of the net radiation R_n with the latent heat of vaporization λ multiplied with the precipitation P , is defined here as the aridity $R_n/\lambda P$. Tree cover is determined as the minimum value of the mean monthly projective cover based on fPar-observations (Donohue et al., 2013). The maximum grass cover was found by subtracting the tree cover from the remotely sensed projective cover.

Study Site	Howard Springs	Adelaide River	Daly River	Dry River	Sturt Plains
FLUXNET ID	AU-How	AU-Ade	AU-DaS	AU-Dry	AU-Stp
Coordinates	12.49S 131.35E	13.08S 131.12E	14.16S 131.39E	15.26S 132.37E	17.15S 133.35E
Prec. (mm year ⁻¹)	1747	1497	1166	898	616
Pot. evap. (mm year ⁻¹)	1763	1802	1896	1948	2082
Aridity. (-)	1.03	1.18	1.48	1.87	2.70
Net Rad. (MJ m ⁻² year ⁻¹)	4392	4313	4215	4105	4079
Mean max. temp. [°C]	37.5	38.8	40.6	41.1	43.0
Mean min. temp. [°C]	27.4	26.6	26.9	27.7	28.1
Tree cover (%)	39.8	20.8	37.5	26.6	7.4
Max. grass cover (%)	44.3	59.2	42.5	49.4	57.6
Species					
Overstorey	<i>Eu. miniata</i> <i>Eu. tetradonta</i> <i>Er. chlorostachys</i>	<i>Eu. tectifera</i> <i>Co. latifolia</i> <i>Pl. careya</i>	<i>Te. grandiflora</i> <i>Eu. tetradonta</i> <i>Co. latifolia</i>	<i>Eu. tetradonta</i> <i>Co. terminalis</i> <i>Eu. dichromophloia</i>	-
Understorey	<i>Sorghum spp.</i> <i>He. triticeus</i>	<i>Sorghum spp.</i> <i>Ch. fallax</i>	<i>Sorghum spp.</i> <i>He. triticeus</i>	<i>Sorghum intrans</i> <i>Th. Tiandra</i> <i>Ch. fallax</i>	<i>Astrelba spp.</i>

200 transpiration (depending on the atmospheric vapour pressure deficit) and hence root water uptake costs and limitations. The vertical distribution in the soil profile of the root surface is optimized in a way to satisfy the canopy water demand with the minimum possible total root surface area.

2.2.2 Long- and short-term optimization

A set of vegetation properties is assumed not to vary considerably over the long-term (20-30 years), and optimized for the
 205 full simulation period. These vegetation properties involve the rooting depths of the perennial trees and the seasonal grasses,



the foliage projected cover of the perennial vegetation, as well as parameters relating to the water use strategies of both the perennial and the seasonal vegetation. Several other vegetation properties are allowed to vary on a daily basis in a way to maximize the daily NCP, such as seasonal vegetation cover, photosynthetic capacities and root surface area distributions of the seasonal and perennial vegetation component.

210 **2.2.3 Water balance model**

The hydrological schematization consists of a permeable block that contains an unsaturated zone and a saturated zone Schymanski et al. (2015), with an impermeable bed with a prescribed drainage level. Here, vertical water fluxes occur between different soil layers. The hydrological parameters were set to resemble freely draining conditions, in absence of more detailed information for each of the sites and for consistency with the simulations of Whitley et al. (2016). Precipitation that falls on
215 the soil block can cause immediate surface runoff or infiltrate, after which it can be taken up by roots, evaporate from the soils, or drain away at a depth of 30m. The simulation of soil evaporation and vertical fluxes in the unsaturated zone are described in Schymanski et al. (2008, 2015).

2.2.4 Model optimization

The vegetation properties (see also Table S6.2 in Supplement S6) are optimized for maximum NCP by the Shuffled Complex
220 Evolution algorithm (SCE, Duan et al., 1994) for the entire simulation period of 37 years (1-1-1980 until 31-12-2017). After an initial random seed, the algorithm subdivides the parameter sets into a number complexes (set here to 10). Afterwards, it performs a combination of local optimization within each complex and mixing between complexes to converge to a global optimum.

2.2.5 Model input and data

225 The meteorological data to run the VOM was obtained from the Australian SILO Data Drill (Jeffrey et al., 2001), as it provided long time series (20-30 years) for the optimization of the VOM. The meteorological data needed for the VOM consists of daily maximum and minimum temperatures, shortwave radiation, precipitation, vapour pressure and atmospheric pressure. Atmospheric CO₂-levels were taken from the Mauna Loa CO₂-records (Keeling et al., 2005). This was preferred to using observed values at the flux tower sites due to the required length of the timeseries for the VOM (20-30 years). See also
230 Supplement S1, Figures S1.1-1.6 for the time series of meteorological data for all sites.

Besides meteorological inputs, the VOM requires soil parameters regarding soil water retentions and hydraulic conductivities for each depth. There were some field measurements of sand, clay and silt content provided by L. B. Hutley and J. Beringer helped describe the composition of the soils in the top 10 cm, whereas values for deeper soil layers were taken from the Soil and Landscape Grid of Australia (Viscarra Rossel et al., 2014a,b,c). The resulting fractions of sand, silt and clay allowed to
235 classify the soils into one of the soil textural groups of Carsel and Parrish (1988), after which the final parameters for the soil water retention model of (Van Genuchten, 1980) and the hydraulic conductivity could be looked up from the accompanying



tables⁶ and used in the VOM. The soil compositions in Whitley et al. (2016) would lead to differences in the soil classifications and represented just the upper layers, but these differences remained rather small. Whitley et al. (2016) reported hydraulic conductivities as well, but the models all used their own methods to determine the hydraulic parameters (see Table 2, Whitley et al., 2016). Moreover, the soil hydraulic conductivities reported by Whitley et al. (2016) were substantially lower than typical values for the reported soil textures (Carsel and Parrish, 1988). At some sites, these low hydraulic conductivities hardly allowed any flow of water and vegetation growth in the VOM. For this reason, for the VOM simulations, soils were solely classified with the field measurements and data of the Soil and Landscape Grid of Australia (Viscarra Rossel et al., 2014a,b,c), whereas the final soil parameters (Table 2) were adopted from Carsel and Parrish (1988).

The flux towers across Australia and New Zealand (OzFlux Beringer et al., 2016) belong to a regional network of the global FLUXNET network and provided time series for the model evaluation. These timeseries consisted of net ecosystem exchange (NEE) of carbon dioxide and latent heat flux (LE), along with the usual energy fluxes and meteorological measurements recorded at OzFlux sites. The flux tower data was processed with the Dingo-algorithm (Beringer et al., 2017), that provided a gap-filled estimation of gross primary productivity (GPP) and latent heat flux (LE). LE was converted to evapo-transpiration (ET), which we define here as the sum of all evaporation and transpiration processes, even though these processes are different in nature (Savenije, 2004). GPP and ET were both used for comparison with the modelled fluxes. The VOM was evaluated for the overlapping time periods of the model time period and the flux tower time period for each site (see Table S6.1 in Supplement S6).

In order to evaluate the foliage cover predicted by the VOM, remotely sensed data of monthly fractions of Photosynthetically Active Radiation absorbed by vegetation (fPAR) from Donohue et al. (2008, 2013) was used to estimate foliage projected cover (FPC) at the different study sites. The maximum possible value of fPAR was defined as 0.95 by Donohue et al. (2008) and relates to maximum projective cover (i.e. FPC = 1.0). At the same time, FPC relates linearly with fPAR-data (Asrar et al., 1984; Lu, 2003), and FPC was thus calculated by dividing the fPAR-values by the maximum value of 0.95.

2.3 Modelling experiments and intercomparison

Several sets of model runs were performed in order to address the different hypotheses. The first hypothesis relates to a model intercomparison with Whitley et al. (2016), whereas the second and third hypothesis was addressed using simulations where some of the prognostic vegetation properties and behaviour were replaced by prescribed values. The last hypothesis was addressed by running a sensitivity analysis for the cost factor of water transport.

2.3.1 Model intercomparison

In a first round of model runs to address the first hypothesis, VOM results were compared to the results of Whitley et al. (2016), who used the terrestrial biosphere models SPA (Williams et al., 1996a), MAESPA (Duursma and Medlyn, 2012), CABLE (Kowalczyk et al., 2006; Wang et al., 2011), BIOS2 (Haverd et al., 2013), BESS (Ryu et al., 2011, 2012) and LPJ-GUESS (Smith et al., 2001) to simulate savannas along the NATT (see also Table 2 Whitley et al., 2016). From these TBMs

⁶see also <https://vom.readthedocs.io/en/latest/soildata.html>



Table 2. Soil characteristics of the study sites along the North Australian Tropical Transect, based on data from the Soil and Landscape Grid of Australia (Viscarra Rossel et al., 2014a,b,c), in addition to field measurements of J. Beringer and L. B. Hutley. Here, θ_r refers to the residual moisture content, θ_s the saturated water content, α and n the Van Genuchten soil parameters (Van Genuchten, 1980) and K_{sat} the saturated hydraulic conductivity.

Howard Springs	Soil type	θ_r (-)	θ_s (-)	α (1/m)	n (-)	K_{sat} (m/s)
0.00-0.20m	Sandy Loam	0.065	0.41	7.5	1.89	$1.228 * 10^{-5}$
0.20-0.40m	Sandy Loam	0.065	0.41	7.5	1.89	$1.228 * 10^{-5}$
0.40-0.60m	Sandy Clay Loam	0.1	0.39	5.9	1.48	$3.639 * 10^{-6}$
0.60-bedrock	Sandy Clay Loam	0.1	0.39	5.9	1.48	$3.639 * 10^{-6}$
Adelaide River						
0.00-0.20m	Silt Loam	0.067	0.45	2	1.41	$1.25 * 10^{-6}$
0.20-0.40m	Sandy Clay Loam	0.1	0.39	5.9	1.48	$3.639 * 10^{-6}$
0.40-0.60m	Sandy Clay Loam	0.1	0.39	5.9	1.48	$3.639 * 10^{-6}$
0.60-bedrock	Sandy Clay Loam	0.1	0.39	5.9	1.48	$3.639 * 10^{-6}$
Daly River						
0.00-0.20m	Sandy Loam	0.065	0.41	7.5	1.89	$1.228 * 10^{-5}$
0.20-0.40m	Loamy Sand	0.057	0.41	12.4	2.28	$4.053 * 10^{-6}$
0.40-0.60m	Sandy Loam	0.065	0.41	7.5	1.89	$1.228 * 10^{-5}$
0.60-bedrock	Sandy Clay Loam	0.1	0.39	5.9	1.48	$3.639 * 10^{-6}$
Dry River						
0.00-0.20m	Sandy Loam	0.065	0.41	7.5	1.89	$1.228 * 10^{-5}$
0.20-0.40m	Sandy Clay Loam	0.1	0.39	5.9	1.48	$3.639 * 10^{-6}$
0.40-0.60m	Sandy Clay	0.1	0.38	2.7	1.23	$3.333 * 10^{-6}$
0.60-bedrock	Sandy Clay	0.1	0.38	2.7	1.23	$3.333 * 10^{-6}$
Sturt Plains						
0.00-0.20m	Silt Loam	0.067	0.45	2	1.41	$1.25 * 10^{-6}$
0.20-0.40m	Sandy Clay	0.1	0.38	2.7	1.23	$3.333 * 10^{-6}$
0.40-0.60m	Sandy Clay	0.1	0.38	2.7	1.23	$3.333 * 10^{-6}$
0.60-bedrock	Sandy Clay	0.1	0.38	2.7	1.23	$3.333 * 10^{-6}$



only LPJ-GUESS uses a carbon allocation scheme to simulate canopy dynamics, whereas the other five models use observed
270 leaf area index to represent vegetation dynamics. Similar to Whitley et al. (2016), the model intercomparison is based on
ensemble timeseries of daily GPP and ET obtained from the different models over the entire duration of flux tower observations
for each site (see Table S6.1 in Supplement S6 for the overlapping model periods with the flux tower observations). Model
performance metrics include relative errors between the mean annual fluxes and the seasonal amplitudes. The study of Whitley
et al. (2016) ranked the models against empirical benchmark models, as originally proposed by Abramowitz (2012). This
275 comparison against calibrated empirical models was not performed here in favour of a more detailed analysis of the actual time
series to provide more insights into model deficiencies relative to the observed vegetation behaviour.

2.3.2 Predicted and prescribed vegetation parameters

To test the second and third hypotheses, regarding the optimality of rooting depths and vegetation cover, we ran model simula-
tions with prescribed rooting depths and/or vegetation cover. The total vegetation cover (perennial and seasonal) was prescribed
280 based on monthly fPAR-data from Donohue et al. (2013), once considering inter-annual variability (i.e. using the actual values
of fPAR-based vegetation cover, gap-filled using monthly ensemble means) and once ignoring inter-annual variability (i.e.
using monthly ensemble means of the full model period). This was done in order to assess if inter-annual variability in vege-
tation cover plays an important role and if that role is captured by optimizing vegetation cover. The perennial tree cover was
estimated as the minimum value of the monthly ensemble means, and then subtracted from the remaining timeseries to obtain
285 the dynamic component of the seasonal grass cover. For Sturt Plains, the perennial cover was set to 0, as prescription of peren-
nial cover corresponding to the minimum value of the monthly ensemble means (0.07) did not allow the SCE-optimization to
converge. See Figure S4.1 for the observed and constructed time series of projective cover at each site. Figure S4.1e) illustrates
that vegetation cover at Sturt Plains reaches almost 0 in many years, but not always in the same month, so that there is no month
with an ensemble mean of 0. This illustrates that the estimation of the evergreen component of cover by taking the minimum
290 monthly ensemble mean may not work well in a climate that lacks a clear seasonality. For the simulation runs with prescribed
rooting depths, we used the same value of 2 m for both trees and grasses, similar to the simulations by LPJ-GUESS in Whitley
et al. (2016).

2.3.3 Sensitivity cost factor for water transport

The cost factor for water transport (c_{rv}) cannot be easily estimated from empirical data, and was initially set to $1.2 \mu\text{mol m}^{-3}$
295 s^{-1} by Schymanski et al. (2009b) after a sensitivity analysis for Howard Springs. Later on, after an adjustment of the water
balance model and another sensitivity analysis at the same site, it was set to $1.0 \mu\text{mol m}^{-3} \text{s}^{-1}$ by Schymanski et al. (2015).
To assess the effect of this cost factor on the simulations more rigorously and test the fourth hypothesis, we ran additional
optimizations with values for c_{rv} ranging from 0.2 to $3.0 \mu\text{mol m}^{-3} \text{s}^{-1}$ for each site along the transect. To test Hypothesis 4,
we analyzed if the value of c_{rv} that best reproduces satellite-derived dry season vegetation cover varies between sites by more
300 than $0.2 \mu\text{mol m}^{-3} \text{s}^{-1}$. Regardless of the result here, we used a c_{rv} value of $1.0 \mu\text{mol m}^{-3} \text{s}^{-1}$, for all other simulations in
this study, similar to Schymanski et al. (2015).

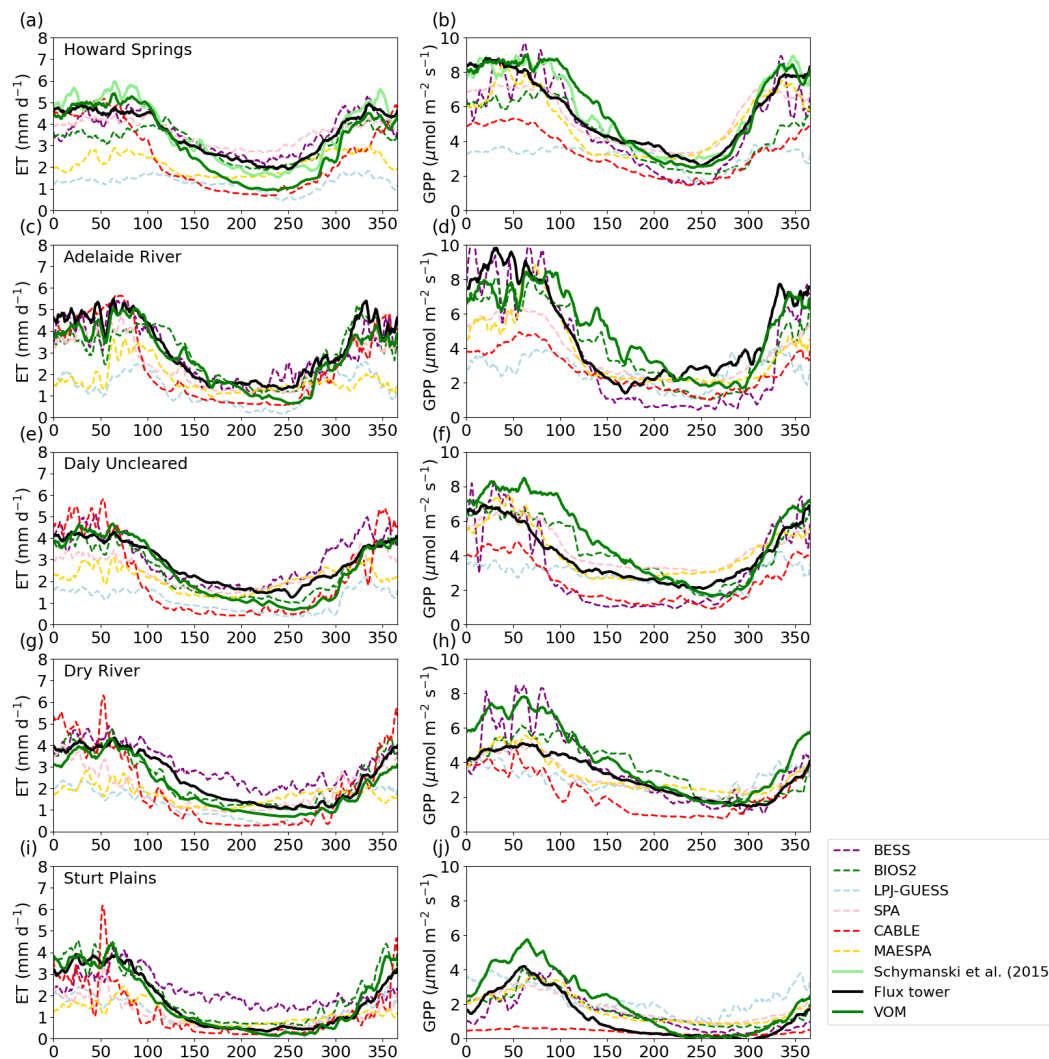


Figure 2. Ensemble years of evapo-transpiration (ET) and gross primary productivity (GPP) for the VOM (darkgreen), flux tower observations (black), results of Schymanski et al. (2015) (lightgreen) and the models BESS (dashed purple), BIOS2 (dashed green), LPJ-GUESS (dashed lightblue), SPA (dashed pink), CABLE (dashed red) and MAESPA (dashed yellow) from Whitley et al. (2016), all smoothed by a 7-day moving average. The ensemble years are calculated for the overlapping time periods with the flux tower observations (see Table S6.1 in Supplement S6).



3 Results

3.1 Model intercomparison - Hypothesis 1

The simulations for the model intercomparison were performed using the same water transport cost factor for all sites as in Schymanski et al. (2015), i.e. $c_{rv} = 1.0 \mu\text{mol m}^{-3} \text{s}^{-1}$. These simulations of evapo-transpiration (ET) by the VOM followed the observed seasonality at the different sites relatively closely, with a tendency to underestimate ET during the dry season at some sites, although to a lesser degree than some of the other models (Fig. 2, left column). Gross primary productivity (GPP), on the other hand, was systematically overpredicted by the VOM during the wet and/or at the transition between wet and dry seasons, making it the worst performing model for GPP for limited periods at some sites (Figure 2, right column). However, in terms of mean annual ET, the VOM belonged to the three best performing models along with BESS and BIOS2 (Figure 3a-b) with on average an off-set from the observations of $102.8 \text{ mm year}^{-1}$ (BESS and BIOS2 with respectively 64.0 and $65.7 \text{ mm year}^{-1}$), whereas the mean annual GPP was better for SPA, MAESPA and BIOS2 with average off-sets of 4.9 , 10.9 and $5.0 \text{ mol m}^{-2} \text{ year}^{-1}$, respectively, compared to the VOM with an average off-set of $18.9 \text{ mol m}^{-2} \text{ year}^{-1}$. The remaining models either strongly underestimated ET or GPP, or both at some sites or throughout the transect. In contrast to the general underestimation of GPP by the other models, the fully optimized VOM-runs showed a tendency to overestimate GPP along the whole transect (except for Adelaide River), whereas VOM-runs with prescribed vegetation cover led to correct values of mean annual GPP at the drier sites, while underestimating GPP at the wetter sites. In terms of relative errors in the mean annual fluxes, the VOM simulations show the most consistently small errors in ET across the transect compared to the other models, except for BIOS2, with a relative error of less than 0.25 across all sites (Figure 3c, on average -0.1 , in comparison with BESS 0.11 , BIOS2 -0.03 , CABLE -0.27 , LPJ-GUESS -0.53 , MAESPA -0.34 and SPA -0.17), while the relative errors in GPP increase with the aridity of the site (Figure 3d) and make the VOM one of the worst performing models in terms of reproducing observed mean annual GPP at the drier sites, resulting in on average a relative error of 0.25 (BESS -0.05 , BIOS2 0.03 , CABLE -0.45 , LPJ-GUESS -0.12 , MAESPA 0.01 and SPA 0.04).

The VOM is among the models with the smallest relative errors for the seasonal amplitude in ET (Figure 3e, with on average a relative error of 0.08), except for Howard Springs and Daly River, where the seasonal amplitude is strongly overestimated mainly due to underestimation of the dry season fluxes. In contrast, most of the other models (CABLE being the exception) tend to strongly underestimate the seasonal amplitude in ET, which is evident in both the ensemble time series (Figure 2) and the relative errors in the seasonal amplitudes (Fig. 3e, with on average a relative error for CABLE of 0.57 , and BESS, BIOS2, LPJ-GUESS, MAESPA and SPA with an error of -0.06 , -0.06 , -0.40 , -0.44 , -0.20 , respectively). The seasonal amplitude of GPP was also overestimated by the VOM (except for Adelaide River), but was on average the smallest of all models (0.09 , whereas BESS, BIOS2, CABLE, LPJ-GUESS, MAESPA and SPA all had errors of 0.32 , -0.15 , -0.37 , -0.46 , -0.12 and -0.30 respectively.) However, the overestimation of the VOM was merely due to overestimated dry season fluxes instead of underestimated dry season fluxes (Figs. 2 and 3f). VOM simulations with prescribed cover largely remove this bias at the drier sites, while leading to opposite errors at the wetter sites. All of the other models underestimate the seasonal signals in GPP,

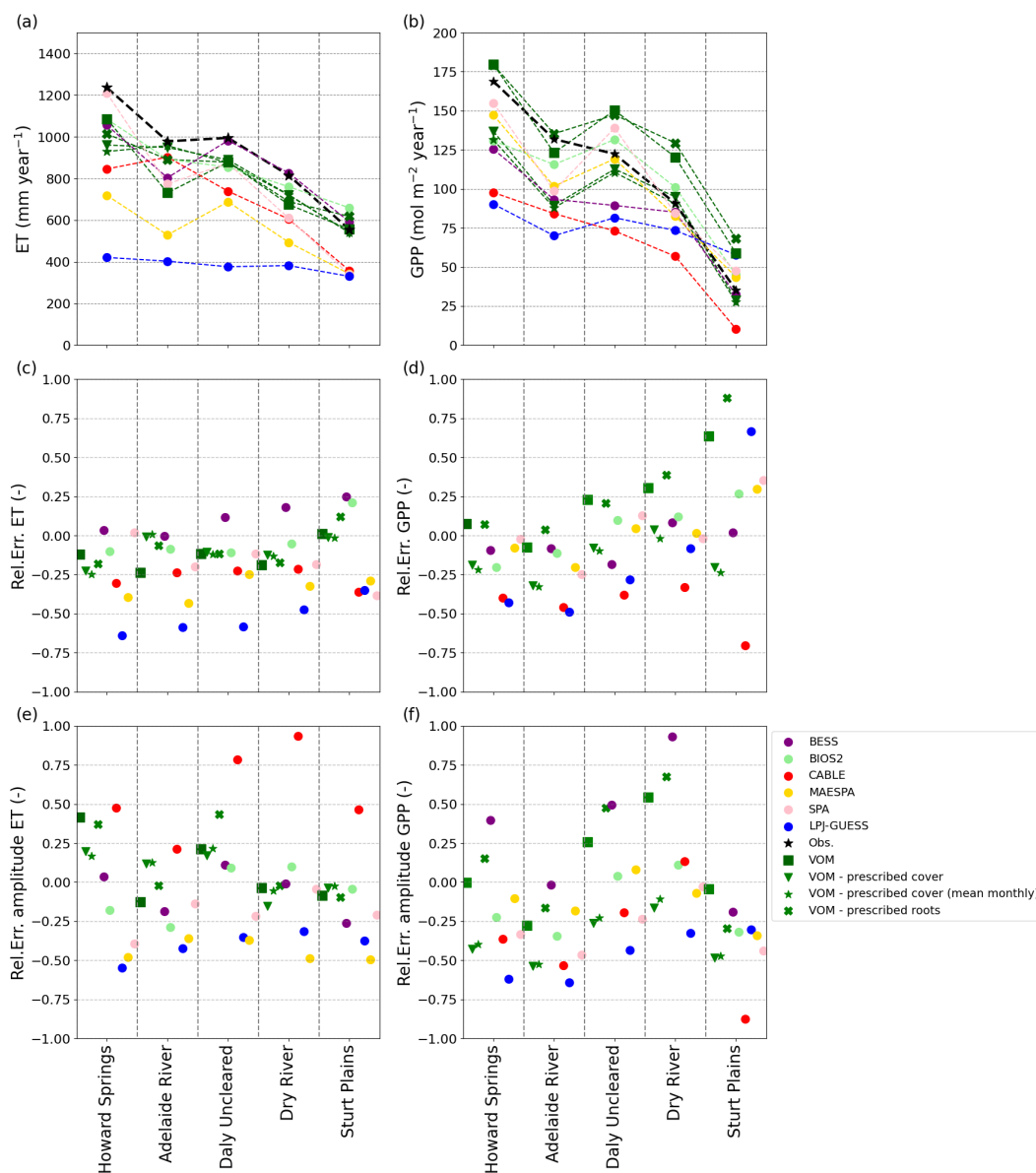


Figure 3. Performance of the VOM and the models analyzed by Whitley et al. (2016) in comparison with flux tower observations. a) and b): Mean annual evapo-transpiration (ET) and gross primary productivity (GPP); c) and d): the relative error of the mean annual ET and GPP; e) and f): the relative error for the mean seasonal amplitude of ET and GPP. All metrics for all models are calculated for the overlapping time period of the model time period and the flux tower time period for each site (see Table Table S6.1 in Supplement S6).

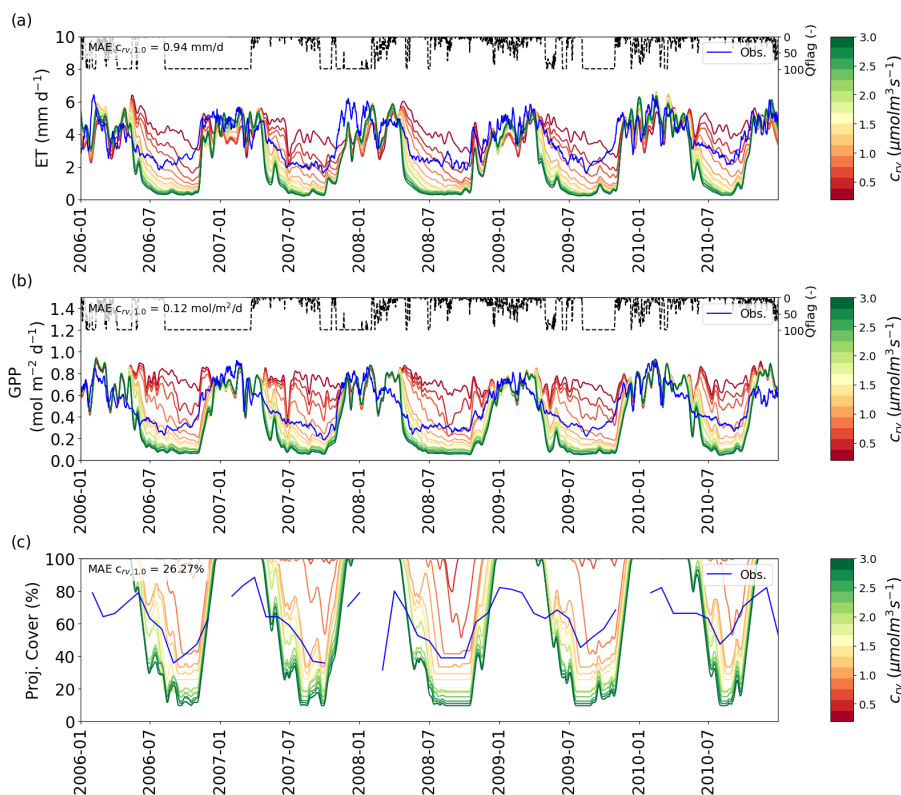


Figure 4. VOM-results for different values of the cost factor c_{rv} (color scale) for Howard Springs for 2006-2010 (as a subset from 1980-2017), with a) the evapo-transpiration (ET), with flux tower observations in blue b) gross primary productivity (GPP), with flux tower observations in blue and c) projective cover, with the observed fraction of vegetation cover based on fPAR-data (Donohue et al., 2013) in blue. The time series for ET and GPP are all smoothed with moving average with a window of 7 days. Daily average quality flags for the flux tower observations are added on top and range from 0 (no missing values) to a 100 (completely gap-filled). In each panel, the mean absolute error (MAE) is given for the simulation with $c_{rv} = 1.0 \mu\text{mol m}^{-3} \text{s}^{-1}$.

335 except for BESS, which overestimates the seasonal signal even more than the VOM for most sites (with an average relative error for BESS of 0.32 and for the VOM of 0.09).

3.2 Sensitivity to carbon costs of plant water transport - Hypothesis 2

In order to investigate the systematic departures of the VOM simulations from observations, we investigated the sensitivity of the results to the cost factor for water transport c_{rv} (see also Supplement S3). The cost factor has a substantial influence on the fluxes (Figure 4), but especially the vegetation cover during the dry season (i.e. the minimum values in Figure 4c) decrease strongly with an increasing cost factor. At all sites, the vegetation cover is very sensitive to the cost factor for values below 1-1.8 $\mu\text{mol m}^{-3} \text{s}^{-1}$ and becomes much less sensitive at higher c_{rv} values (Figs. 5a-e).

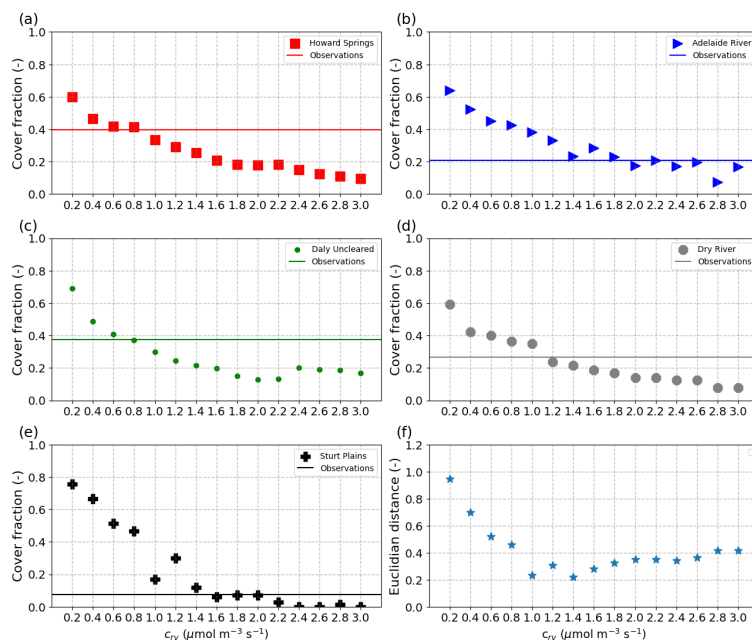


Figure 5. Simulated dry season percentage vegetation cover at each site (a-e) and the Euclidian distance of errors between sites (f) as a function of the water transport system cost factor (c_{rv}). Symbols illustrate simulated fractional cover of perennial vegetation ($M_{a,p}$), while solid lines illustrate the perennial tree cover derived from observations, as described in Sect. 2.3.2. The Euclidean distance in panel f) was based on the error between observed and simulated vegetation fraction during the dry season for all five study site, i.e. $ED = \sqrt{\sum_{i=1}^n E_i^2}$, with E_i the error for each site for a given c_{rv} .

The decrease in persistent vegetation cover with increasing values of c_{rv} was not always smooth in our simulations (Fig. 5a-e). Therefore, when optimizing for the c_{rv} value that most closely reproduces observed dry season FPC (solid lines in Fig. 5a-e), visual interpolation of the dots would result in a range of candidate values for each site. For example, at Howard Springs, the best value would be somewhere between 0.6 and 1.0 $\mu\text{mol m}^{-3} \text{s}^{-1}$, at Adelaide River anywhere between 1.4 and 2.6, at Daly River between 0.8 and 1.0, at Dry River between 1.0 and 1.2, and at Sturt Plains between 1.4 and 2.0 $\mu\text{mol m}^{-3} \text{s}^{-1}$. Conversely, if we were to choose the same value for all sites along the transect, then a value of 1.4 $\mu\text{mol m}^{-3} \text{s}^{-1}$ would minimize the Euclidian distance based on the error for all five study sites (Figure 5f), closely followed by the value of 1.0 $\mu\text{mol m}^{-3} \text{s}^{-1}$.

3.3 Predicted and prescribed foliage cover - Hypothesis 3

The VOM predicted that projective cover would reach 100% during the wet season at all sites, but observed maximum values of cover ranged between 60% and 80% for the different sites (see e.g. Fig. 4c for Howard Springs, see Supplement S2 Figures S2.1, S2.4, S2.7, S2.10, S2.13 for the other sites). At the same time, carbon uptake rates during the wet season were overpredicted at most sites by the VOM (Fig. 2), which prompts the question if the overprediction of projective cover might be linked to the



overprediction of carbon uptake. To test this hypothesis, the VOM simulations were repeated with prescribed foliage projective cover based on observed fPAR-data (Donohue et al., 2013), while everything else was optimized as usual (see for the full analysis Supplement S4).

When prescribing fractional tree cover to the value of 0.07 derived from observed dry season cover at Sturt Plains (Supplement S4, Fig. S4.1e), the Shuffled Complex Evolution (SCE) algorithm did not converge, i.e. no parameter sets resulting in positive net carbon profit (NCP) were found. Only when the tree cover and tree rooting depths were set to zero and all the observed cover was interpreted as grass cover (consistent with the fact that the site is an extensively grazed grassland) the SCE found optimal water use strategy parameters for the grasses, resulting in a positive maximum NCP.

In general, prescribing vegetation cover in the VOM consistently reduced the mean annual GPP at all study sites (Figure 6b), which led to a shift in the average off-set from the observations from +18.9 to -18.7 mol m⁻³ s⁻¹. This happens most strongly during the wet season (Figure 6d), as expected, and during the transition to the dry season (Figure 6h). During this transition from the wet to the dry season (April-May, Figures 6g,h), prescribing cover indeed improved the simulations for all sites, whereas the reductions in the wet season resulted in an underprediction of GPP at all sites (Fig. 6d). Even in the dry season, prescribed cover reduced simulated GPP and improved the match with observations, except for one site (Dry River, Fig. 6f). The effect on evaporation was less pronounced, as reduced cover led to reduced transpiration, but this was partly compensated for by increased bare soil evaporation (Fig. 6a, c, e, g, i).

Looking at the fluxes in more detail and taking Daly River as an example (Figure 7), we see that the initial overestimation of GPP during the transition from the wet to the dry season is largely eliminated when projected cover dynamics are prescribed based on remote sensing observations, but merely caused by generally lower GPP rates and at the cost of underestimating GPP during the early wet season. Similar patterns can be seen for the other sites in Supplement S4, Fig. S4.2-4.6, except for Dry River and Sturt Plains, where the wet seasons are shifted more towards the middle of the year. At Dry River (Supplement, Fig. S4.5), prescribed cover captured wet season GPP much better than predicted cover, while it overestimated dry season fluxes compared to observations and simulations based on predicted cover. The plots in Supplement S4 also illustrate that the two different ways of prescribing vegetation cover, with and without inter-annual variability, only led to marginal differences in the simulated fluxes.

3.4 Predicted and prescribed rooting depths - Hypothesis 4

To assess if optimization of rooting depths in the VOM has any effect on predicting fluxes, we compared the original simulations, that optimized rooting depths, with simulations based on prescribed rooting depths. The optimized grass rooting depths were all similar at around 0.5 m over the entire transect, and tree rooting depths varied between 0.6 and 2.2 m (Figure 8a and b), whereas rooting depths of 2 m for trees and grasses alike were prescribed in the new simulations. Even though there was a decreasing pattern of the optimized tree rooting depths over the transect (shallower roots towards drier sites), prescribing rooting depths did not lead to substantially different mean annual evapo-transpiration and gross primary productivity in comparison with the optimized VOM (Figure 3a and b) with deviations from the observed mean annual values of respectively -102.8 mm year⁻¹ and 97.8 mm year⁻¹. Only mean annual GPP slightly increased for the drier sites if rooting depths of 2

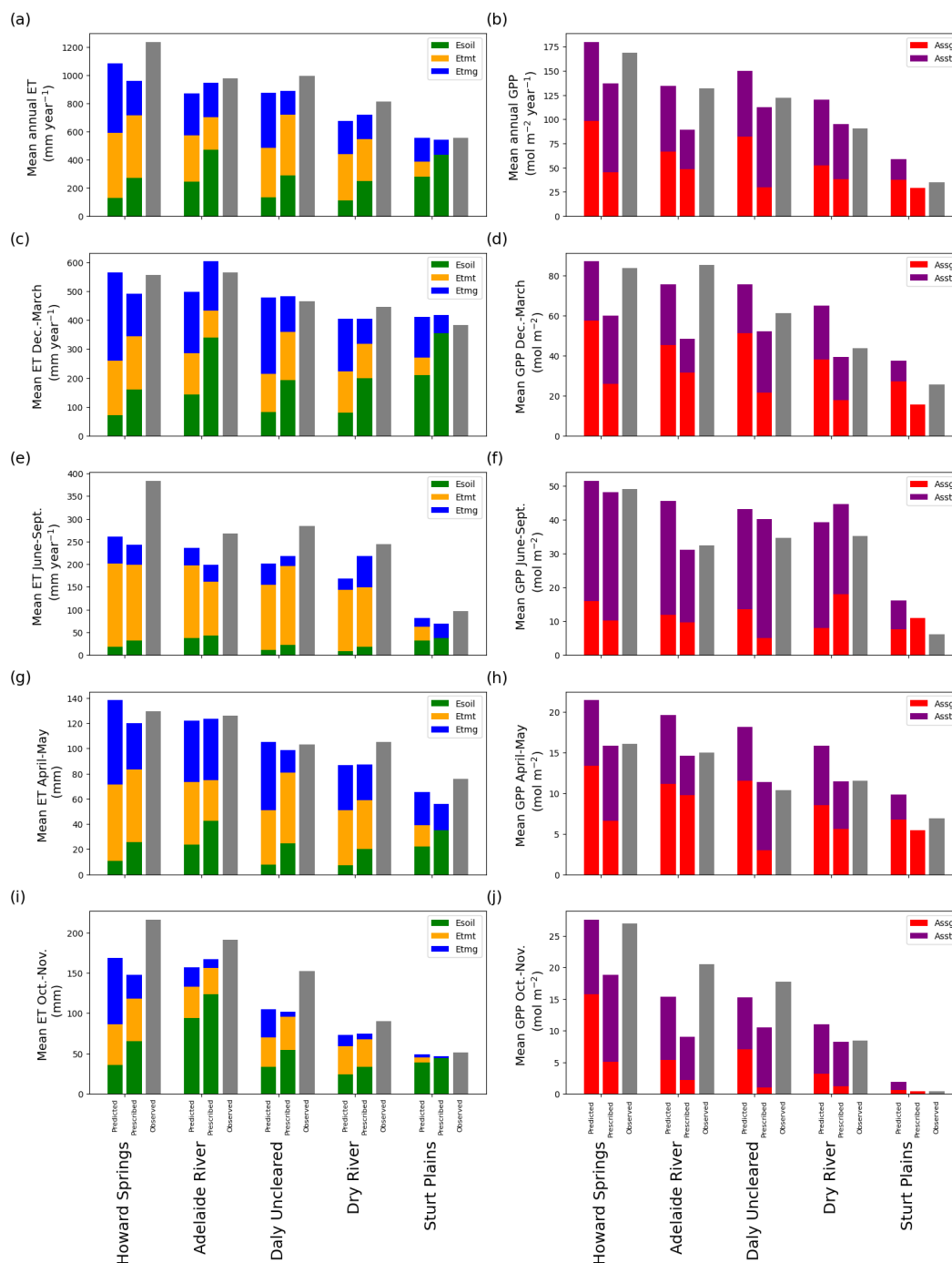


Figure 6. Observed and predicted fluxes of water and CO₂ using prognostic or prescribed cover at the different sites. Simulated evapotranspiration (ET) was sub-divided into soil evaporation (green), tree transpiration (orange) and grass transpiration (blue), while simulated gross primary productivity (GPP) was subdivided into that of trees (red) and grasses (purple). Observations are shown as gray bars. Panels c) and d) represent the fluxes for December-March (generally the wet season), e) and f) the flux partition for June - September (i.e. generally the dry season), and g) and h) the fluxes for April-May (i.e. generally the transition from the wet to the dry season), and i) and j) the fluxes for October-November (i.e. generally the transition from the dry to the wet season). All metrics for all models are calculated for the overlapping time period of the model time period and the flux tower time period for each site (see Table S6.1 in Supplement S6).

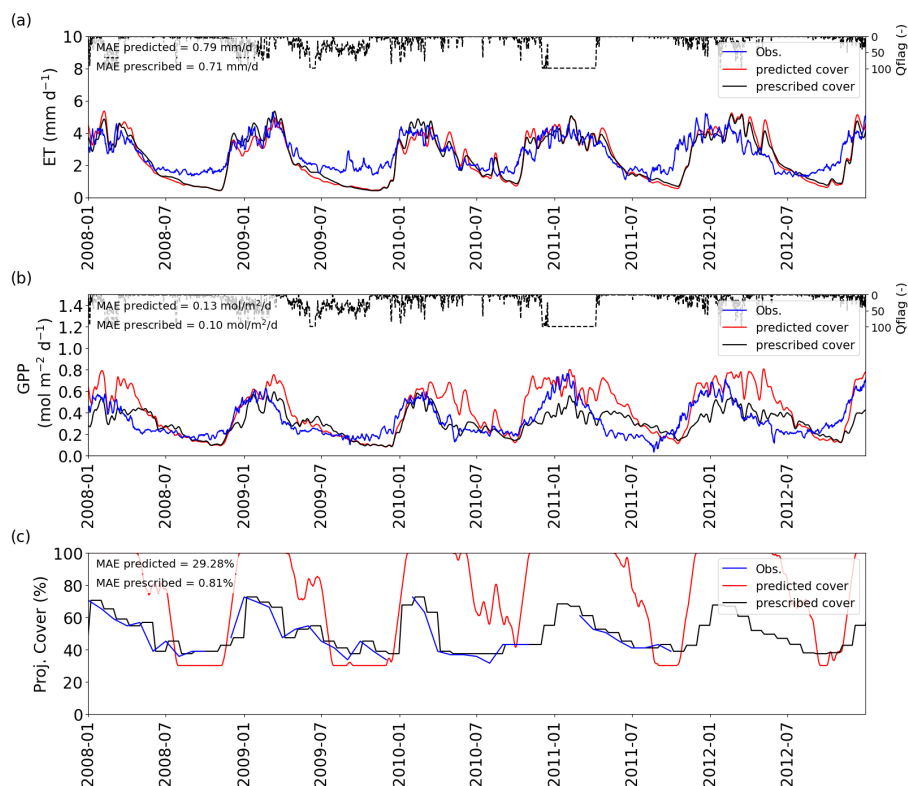


Figure 7. Comparison between the VOM with prescribed and predicted vegetation cover for Daly River for 2008-2012 (as a subset from 1980-2017), for a) evapo-transpiration (ET) and b) gross primary productivity (GPP) and c) projective cover, with model results obtained by the predicted cover in red and the prescribed cover in black. The flux tower observations and fPAR-derived projective cover are shown in blue. Daily average quality flags for the flux tower observations are added on top and range from 0 (no missing values) to a 100 (completely gap-filled). The time series for ET and GPP are all smoothed with a moving average with a window of 7 days.

390 m were prescribed. However, there are clear effects of prescribing 2 m rooting depth at the seasonal scale. The prescribed rooting depths result in increased transpiration and GPP rates in the early dry season, followed by strongly reduced fluxes in the late dry season, compared with simulations based on optimized root depths, as can be seen in Figure 9 for Dry River, as an example, but as also illustrated for the other sites in Supplement S5, Figures S5.1-5.5. Figure S3.8 in Supplement S3 indicates a decreasing sensitivity of the predicted rooting depths to the cost factor for water transport c_{rv} with decreasing mean annual
 395 rainfall along the transect. For example, predicted tree rooting depths at Howard Springs ranged between 1 and 8 m when c_{rv} was varied by an order of magnitude, whereas Sturt Plains only had a variability between 3 m and 1 m for the same range of c_{rv} . Similar to fractional cover (Fig. 5), the predicted rooting depths became less sensitive to c_{rv} above a value of around 1-1.5 $\mu\text{mol m}^{-3} \text{s}^{-1}$.

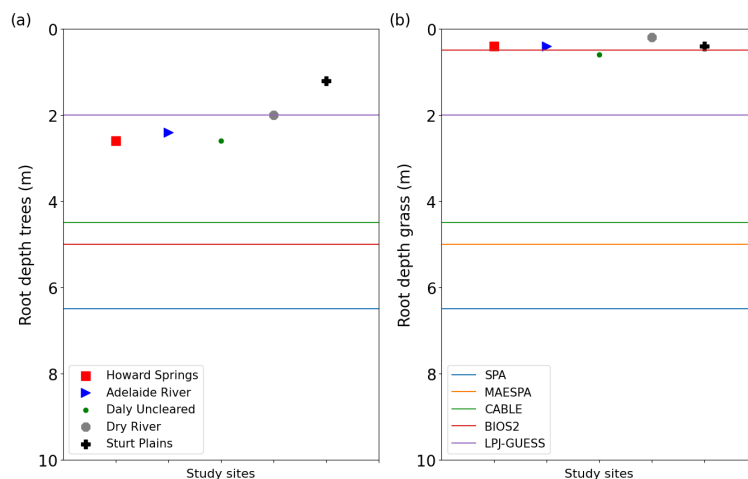


Figure 8. Modelled rooting depths for a) trees and b) grasses, for Howard Springs (red squares), Adelaide River (blue triangles), Daly River (green circles), Dry River (grey octagon), and Sturt Plains (black cross). The colored lines represent the rooting depths of the models used in Whitley et al. (2016) with SPA (blue), MAESPA (orange), CABLE (green), BIOS2 (red) and LPJ-GUESS (purple).

4 Discussion

400 In comparison with the models tested at the same sites by Whitley et al. (2016), the VOM was one of the most robust at capturing water vapour and CO₂ fluxes and their seasonality along the transect. This is surprising, considering that most of the other models used observed seasonal variations in vegetation cover and other site-specific vegetation input, while LPJ-GUESS was the only other model that predicted vegetation dynamics. LPJ-GUESS, however, was not able to reproduce the seasonal amplitude of the fluxes at all and severely underestimated mean annual fluxes throughout the transect, except for an
405 overestimation of GPP at the driest site. According to Whitley et al. (2016), the failure of LPJ-GUESS to capture observed seasonality can be explained by how carbon is allocated in the model on an annual basis, in addition to the empirical prescription of phenology. In contrast, the VOM predicted phenology dynamically from day to day, and had resulting fluxes that showed a much more pronounced seasonal signal, which also corresponded more to the observed flux tower observations.

However, the simulations also revealed some persistent shortcomings of the VOM, e.g. a systematic underestimation of dry
410 season evapo-transpiration (ET) and a systematic overestimation of wet season GPP, accompanied by an overestimation of vegetation cover during the wet season. Possible reasons for these shortcomings and potential ways forward will be discussed below, along with the hypotheses formulated in the introduction.

4.1 Effect of hydrological setting

Our results suggest that the hydrological setting at the different sites, especially the position of the groundwater table, influence
415 the performance of the VOM. The model underestimated evapo-transpiration (ET) during the dry season at all sites, especially in the late dry season. At Howard Springs, this was linked to the lack of a groundwater table in the present simulations, which

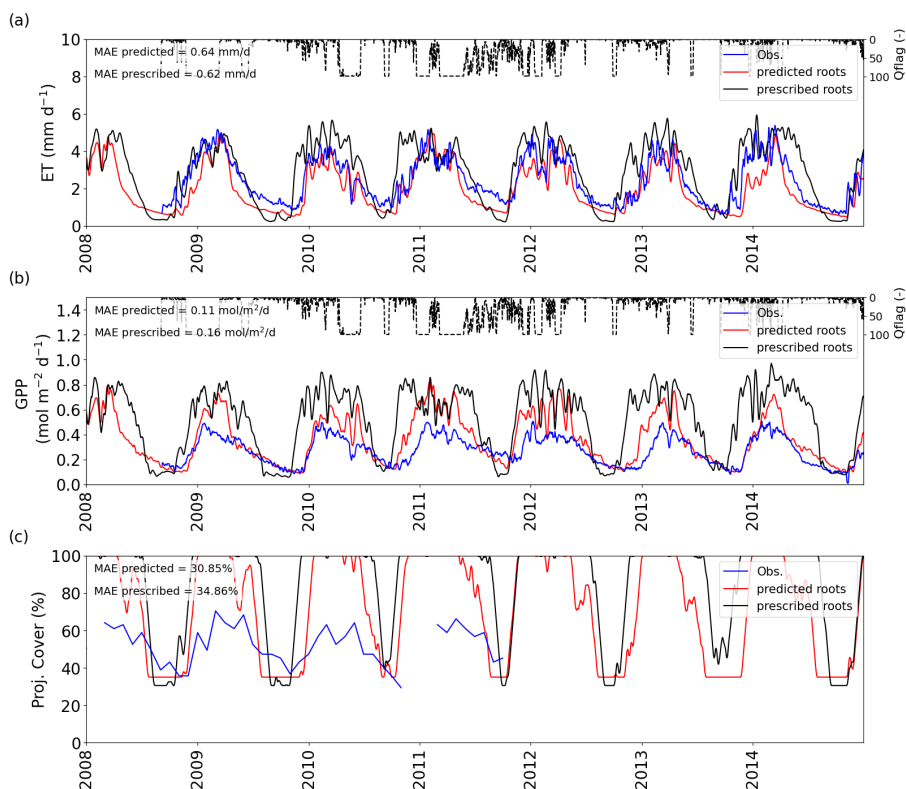


Figure 9. VOM-results for prescribed (black) and predicted (red) rooting depths for Dry River for 2008-2013 (as a subset from 1980-2017), with a) the evapo-transpiration (ET), with flux tower observations in blue b) gross primary productivity (GPP), with flux tower observations in blue and c) projective cover, with the observed fraction of vegetation cover based on fPAR-data (Donohue et al., 2013). Daily average quality flags for the flux tower observations are added on top of a) and b) and range from 0 (no missing values) to a 100 (completely gap-filled). The time series for ET and GPP are all smoothed with moving average with a window of 7 days.

were based on the assumption of freely draining conditions, for compatibility with the previous model intercomparison by Whitley et al. (2016). Previous model applications of the VOM (Schymanski et al., 2009b, 2015), which simulated a variable groundwater table based on local topography at Howard Springs, did not suffer from such a strong underestimation of dry
420 season fluxes (see the accompanying technical note of Nijzink et al. (2021)).

This emphasizes the importance of a correct hydrological parameterization and confirms previous findings that groundwater can have a strong influence on the land surface fluxes (e.g. York et al., 2002; Bierkens and van den Hurk, 2007; Maxwell et al., 2007). It is likely that the role of the hydrological parameterization is more important for the wetter sites along the transect, as greater input of precipitation during the wet season implies a greater potential for soil moisture carry-over into the dry
425 season. Unfortunately, groundwater data was not available in the close vicinity of the other sites of the transect, even though boreholes near the drier sites of Daly River (approx. 2 km distance), Dry River (approx. 13 km) and Sturt Plains (approx. 10 km) suggested deeper groundwater tables for these sites (Supplement S2, Figures S2.8, S2.11, S2.14).



4.2 Predicted foliage cover

Using the same cost factor for the water transport system (c_{rv}) across all sites, the predicted perennial vegetation cover fraction
430 was between 0.3 and 0.4 at all sites except for the driest, grassland site, where it was still predicted at almost 0.2. This is in
contrast to the observed dry season foliage projected cover (FPC), which ranged between 0.07 at the driest and roughly 0.4 at
the wettest site (Figure 5), where Adelaide River was an outlier with only 0.2 FPC in the dry season. The strong over-prediction
of perennial vegetation cover at the driest site, Sturt Plains, might relate to a low sensitivity of the net carbon profit (NCP) to
perennial cover at this site and the fact that it is a lightly grazed grassland site (Hutley et al., 2011). The NCP-values are
435 generally low here (see also Supplement S4, Figure S4.11), and there is only a small difference in NCP between the predicted
optimal tree cover of 16.9% and a forced perennial cover of 0.0 (921.56 and 726.9 mol m⁻² respectively, Supplement 4, Fig.
S4.11). VOM-simulations with prescribed seasonal cover and a forced tree cover of 0.0 resulted in an even smaller NCP of
397.7 mol m⁻², while prescribing perennial cover with 7% and seasonal vegetation cover with the remaining observed cover
yielded only negative NCP-values. Due to the large inter-annual variability at this site and relatively short period of time
440 with observed cover (see Supplement S4, Fig. S4.1e), for the largest part of the modelling period the prescribed cover just
represented the long-term mean monthly values of fPAR-based observations, which is likely far off the actual values. Note
also that a nearby ungrazed woodland site had a dry season leaf area index (LAI) of 0.4 (Hutley et al., 2011) which is roughly
consistent with the predicted fractional cover of 0.2 and assumed clumped LAI within vegetated patches of 2.5 (Schymanski
et al., 2009b).

445 We found that different values of the cost factor for water transport (c_{rv}) could be chosen for each site to best reproduce
observed dry season FPC, but these values would not at the same time improve the match with observed mean annual fluxes, and
in fact, for most sites, different c_{rv} values would need to be chosen to reproduce either mean annual ET or GPP (Supplement
S3, Fig. S3.1). However, the value of c_{rv} affects dry season fluxes much more than wet season fluxes (Figure 4), so adjusting
 c_{rv} to match observed mean annual fluxes would mean that an overestimation of fluxes during the wet season would be
450 compensated by an underestimation during the dry season. Furthermore, comparison between the optimum c_{rv} for Howard
Springs in this study (0.6-0.8 μmol m⁻³ s⁻¹) with the value of 1.0 μmol m⁻³ s⁻¹ obtained by Schymanski et al. (2015), who
considered groundwater influence, suggests that the variation in the best c_{rv} between sites may also be due to different levels
of misrepresentation of the hydrological settings. Neglecting an existing groundwater influence, for example, would result in
lower vegetation cover in the dry season, which could be compensated for by lowering c_{rv} . Similarly, an overestimated soil
455 water holding capacity in the model would result in overestimated dry season vegetation cover and could be compensated for
by a high c_{rv} , leading effectively to the points in Figure 5 being too far to the right. This emphasizes the need for a more
thorough understanding of the carbon costs related to the water transport infrastructure and their dependence on environmental
conditions, including effects of temperature or water stress on the efficiency of plant hydraulics (Roderick and Berry, 2001;
Mencuccini et al., 2007; Hacke et al., 2001).

460 Another issue is that the VOM consistently overestimates vegetation cover in the wet season at all sites, always reaching
100%, which is not consistent with observations. Schymanski et al. (2009b) already pointed out that observed vegetation



cover at Howard Springs did never reach 100% and explained this by seasonal lagoons within the remote sensing grid cell, implicating a low-bias in the remotely sensed vegetation cover. However, in the present study we found that observed vegetation cover never reaches 100% at any of the five sites, while the simulations always do. At the same time, an overprediction of GPP
465 at the drier sites was removed when prescribing vegetation cover based on observations, rather than predicting it based on optimality principles (Figure 6). This suggests that there might be a fundamental bias in the VOM's representation of the costs and benefits of foliage. In the VOM, the relation between leaf area and vegetation cover is assumed to be linear, but this relationship is highly non-linear in reality (Choudhury, 1987). Due to this linear representation of a non-linear function, the carbon costs for high values of vegetation cover are likely underestimated in the VOM, which could be the reason for
470 overestimated wet season vegetation cover. However, note that prescribed vegetation cover led to an underestimation of GPP at the wetter sites, so there is likely still an issue with the translation between the modelled vegetation cover and that derived from remotely sensed fPAR.

4.3 Predicted rooting depths

Rooting depths predicted by the VOM are mostly smaller than those prescribed in the different models studied by Whitley
475 et al. (2016) (Fig. 8a-b), and decrease with decreasing mean annual precipitation along the transect. This is consistent with the findings of Schenk and Jackson (2002), who, based on a large global dataset, also suggested that rooting depths decrease with decreasing mean annual precipitation. In fact, the empirical relation between rooting depths and mean annual precipitation proposed by Schenk and Jackson (2002, Fig. 7), when extrapolated to the mean annual precipitation range of 600-1700 mm/year for the NATT sites, would predict rooting depths between 1.5 and 3.4 m, which is relatively close to the range predicted by
480 the VOM (1.2-2.6 m Figure 8a, or up to 4.2 m when considering groundwater influence in Schymanski et al. (2015)). This suggests that optimizing vegetation parameters for Net Carbon Profit enables predicting a realistic spatial variation in rooting depths. Note, however, that rooting depths are species-dependent and should be expected to also depend on local hydrological conditions, most notably the distance to the water table (Kollet and Maxwell, 2008). Hence any misrepresentation of the hydrological settings in the VOM would result in a biased prediction of rooting depths. Whitley et al. (2016) argued that
485 transpiration rates were maintained relatively high during the dry season due to the presence of deep roots, which is in line with studies suggesting that Eucalypt trees in Northern Australia are deep rooted and therefore maintain high transpiration rates during the dry season (O'Grady et al., 1999; Eamus et al., 2000). As discussed above, the position of the water table was not captured in this set of VOM simulations, so we should not expect that the model would accurately predict rooting depths at the different sites. Yet the VOM provides a non-trivial and encouraging confirmation of the observed trends of increasing rooting
490 depths of perennial vegetation with increasing rainfall. Nevertheless, the rooting depths of grasses were more or less constant along the transect, which contrasts with the changing understorey species composition along the transect. Only at Howards Springs annual *Sorghum* grasses are dominant, whereas a reduction of *Sorghum* grasses and a shift towards more perennial grasses with deeper roots exists with declining precipitation amounts over the transect (Ma et al., 2013). It could be argued that the grass rooting depths at the wetter sites are too deep, as annual *Sorghum* generally reaches depths of around 0.15 m in stead
495 of 0.20 m - 0.60 m for especially the sites of Howard Springs, Adelaide River and Daly River (Fig. 8b). The more frequent fires



at these sites may play a role here, as more long-lasting and deeper rooting grasses are able to develop at the drier sites with less fires. At the same time, the predicted grass rooting depths were similarly sensitive to the cost factor of the water transport system (c_{rv}) as the predicted tree cover, which emphasizes also the importance of a better understanding of these costs for our ability to correctly predict rooting depths and vegetation cover.

500 To test our hypothesis that optimized rooting depths will not result in better reproduction of fluxes than prescribed, homogeneous rooting depths along the transect, VOM-simulations were run with 2 m rooting depth at each site, which is the same rooting depth as assumed for the LPJ-GUESS runs in Whitley et al. (2016). Note that the optimized tree rooting depths (Figure 8a) are in most cases larger than the prescribed values of 2 m, which helps the plants in the VOM to maintain transpiration and GPP during the dry season. At Howard Springs, for example, values drop much lower in the dry season for both evaporation and gross primary productivity when roots are prescribed (Supplement S5, Figure S5.1). Optimized grass rooting depths, in contrast, are much shallower (ca. 0.5 m) than the prescribed 2 m. This results in reduced overall transpiration and gross primary productivity during the early dry season when grasses are still active, compared to simulations with prescribed rooting depths at most sites. At Dry River (Figure 9), where predicted and prescribed tree rooting depths were similar, it becomes obvious that the prescribed 2 m rooting depths for grasses enhance total transpiration during the early dry season at the cost of severely reduced transpiration in the late dry season, when the trees seem to be running out of water. Interestingly, at this site, both simulations underestimate dry season evapo-transpiration, one in the early dry season, the other in the late dry season. In general, however, predicted rooting depths improve simulations of dry season GPP over the transect (see Supplement S5, Figure S5.6f).

515 It can be noted as well that predicted rooting depths result in less biased simulations of foliage projected cover (see Figure 9c as an example). When rooting depth is prescribed to 2 m, full cover is maintained longer into the dry periods, which leads to an overestimation of fluxes compared to observations. This suggests that the effect of prescribing a wrong rooting depth could be partly compensated for by prescribing the correct dynamics of projected cover.

5 Conclusions

Below, we address the original hypotheses of our study, followed by general conclusions.

520 1. The optimality-based model is not substantially worse at capturing the seasonal amplitudes and mean annual values of observed carbon and water fluxes than conventional models analyzed by Whitley et al. (2016) along the NATT.

To our surprise, the maximum Net Carbon Profit principle enabled the Vegetation Optimality Model (VOM) to capture the seasonal amplitudes and mean annual values of carbon and water fluxes along the North Australian Tropical Transect (NATT) to a similar or better degree than conventional models. The VOM showed a strong seasonal signal, in contrast to several other models that generally underestimated the seasonal amplitude of the fluxes. This is remarkable and promising, considering that many vegetation properties are predicted by the VOM, such as tree cover, rooting depth and grass phenology, which have to be prescribed in most of the other models. Therefore, we can conclude that optimality-driven models provide a promising way to model savanna ecosystems.



2. Replacing predicted vegetation cover in the VOM by remotely sensed vegetation cover does not lead to a better reproduction of observed seasonal amplitudes and mean annual fluxes.

530 In the fully prognostic mode, the VOM overestimated GPP during the transition from wet to dry seasons at all sites, which was corrected if vegetation cover was prescribed based on observations. This indicates a rejection of the hypothesis, but, on the other hand, observation-based cover underestimated GPP at the wetter sites in all seasons, leading to a worse bias at these sites than in the fully prognostic model runs. The predicted vegetation cover showed similar dynamics to the observed, but was also systematically overestimated during the wet season (reaching 100% at all sites). Therefore, this
535 hypothesis can not be fully accepted nor rejected, but we also gained new insights by this (see below).

3. Using a prescribed, homogeneous rooting depth in the VOM instead of prognostic rooting depths leads to a worse reproduction of observed seasonal amplitudes and mean annual fluxes.

The optimality-based prognostic rooting depths reproduced carbon and water fluxes better than a prescribed, homogeneous rooting depth of 2 m for all sites. Predicted tree rooting depths were generally deeper than the prescribed, leading
540 to less decrease in the fluxes during the dry season in comparison with prescribed rooting depths. At the same time, predicted grass rooting depths (<0.5 m) were much shallower than the prescribed and reproduced the observed decay in grass fluxes better. The predicted values of tree rooting depths also decreased with mean annual precipitation as observed elsewhere in the literature, indicating the capability of the VOM to provide realistic predictions of rooting depths. Hence, this hypothesis was accepted.

4. Re-calibration of the water transport cost parameter to reproduce remotely sensed dry season vegetation cover at each site will not result in large variation (more than $0.2 \mu\text{mol m}^{-3} \text{s}^{-1}$) of this parameter between sites.

Observed variations in dry season foliage projected cover could be reproduced better if the water transport cost parameter was varied between 0.8 and $2.0 \mu\text{mol m}^{-3} \text{s}^{-1}$, but this would not necessarily lead to improved reproduction of observed fluxes. We found that the representation of hydrological conditions plays an important role here (see below), therefore
550 we can neither confirm nor reject this hypothesis at present.

Since the VOM does not rely on calibration or information about site-specific vegetation properties, we were also able to pinpoint systematic shortcomings that indicate a path to additional research promising to substantially improve our capability to predict responses of savanna systems to environmental change:

- One of these shortcomings relates to the representation of the site-specific hydrological conditions. Due to lack of
555 information about local drainage conditions, the model was parameterized as free draining, resulting in underestimated dry season water use. Further research into a better representation of groundwater dynamics at such sites would likely improve our ability to simulate dry season fluxes.
- Another shortcoming relates to the understanding of trade-offs related to the water transport infrastructure. The transport of water from deep soil layers upwards and its distribution over the foliage requires a sophisticated water transport



560 infrastructure, which is likely linked to substantial carbon costs for its construction and maintenance. We found that the simulations of fluxes especially in the dry season are very sensitive to the parameterization of these costs and more research into their quantification and relation to environmental conditions will likely further improve our modelling capabilities of savanna systems.

– A third shortcoming relates to the representation of carbon costs with respect to foliage. The linear relationship between
565 leaf area and absorbed radiation in the current model, in combination with the neglect of leaf reflectivity results in underestimated carbon costs of maintaining a canopy that can absorb all the light and hence overestimated fraction of absorbed radiation and GPP in the wet season. A better representation of these costs will likely remove the systematic wet season bias discovered in this study.

We conclude that the optimality-based model performed surprisingly well in comparison with more empirically-based con-
570 ventional models, with the additional promise of performing equally well when predicting vegetation responses to yet unseen conditions, as its underlying principles are unlikely to change as the environment changes. Furthermore, the model's independence from calibration and local observations as input enabled us to discover systematic biases and room for improvement that would otherwise be obscured by adjusting parameters to local conditions.

Code and data availability. Model code is available on github (<https://github.com/schymans/VOM>) and the full analysis including all scripts
575 and data are available on renku (<https://renkulab.io/gitlab/remko.nijzink/vomcases>). Before final publication, static versions of these repositories will be uploaded to zenodo.org and receive a separate DOI.

Author contributions. SJS and RN designed the set-up of the study. Model code was originally developed by SJS, but updated and modified by RN. RN did the pre-processing, modelling and post-processing. LH and JB provided site-specific knowledge and data. The main manuscript was prepared by RN, together with input from SJS. LH and JB provided corrections, suggestions and textual inputs for the main
580 manuscript.

Competing interests. The authors declare no conflict of interest

Acknowledgements. This study is part of the WAVE-project funded by the Luxembourg National Research Fund (FNR) ATTRACT programme (A16/SR/11254288).

We would like to acknowledge Rhys Whitley, Vanessa Haver, Martin de Kauwe and Longhui Li for providing the data from Whitley et al.
585 (2016).



This work used eddy covariance data collected by the TERN-OzFlux facility (<http://data.ozflux.org.au/portal/home>). OzFlux would like to acknowledge the financial support of the Australian Federal Government via the National Collaborative Research Infrastructure Scheme and the Education Investment Fund.

We acknowledge the SILO Data Drill hosted by the Queensland Department of Environment and Science for providing the meteorological data (<https://www.longpaddock.qld.gov.au/silo/>).

We acknowledge the Scripps CO₂ program (https://scrippsco2.ucsd.edu/data/atmospheric_co2/primary_mlo_co2_record.html) for the Mauna Loa Observatory Records.

We also acknowledge CSIRO for the Soil and Landscape Grid of Australia (<https://aclep.csiro.au/aclep/soilandlandscapegrid/index.html>) and the Australian monthly fPAR derived from Advanced Very High Resolution Radiometer reflectances - version 5 (<https://data.csiro.au/dap/landingpage?pid=csiro:6084>).

We acknowledge the Northern Territory Water Data WebPortal for the groundwater data (<https://water.nt.gov.au/>).



References

- Abramowitz, G.: Towards a public, standardized, diagnostic benchmarking system for land surface models, *Geoscientific Model Development*, 5, 819–827, <https://doi.org/10.5194/gmd-5-819-2012>, <https://www.geosci-model-dev.net/5/819/2012/>, 2012.
- Allen, R. G., Pereira, L. S., Raes, D., and Smith, M.: Crop evapotranspiration - Guidelines for computing crop water requirements, *Irrigation and drainage paper 56*, FAO - Food and Agriculture Organization of the United Nations, Rome, 1998.
- 600 Asrar, G., Fuchs, M., Kanemasu, E. T., and Hatfield, J. L.: Estimating Absorbed Photosynthetic Radiation and Leaf Area Index from Spectral Reflectance in Wheat1, *Agronomy Journal*, 76, 300, <https://doi.org/10.2134/agronj1984.00021962007600020029x>, <https://www.agronomy.org/publications/aj/abstracts/76/2/AJ0760020300>, 1984.
- Baudena, M., Dekker, S. C., van Bodegom, P. M., Cuesta, B., Higgins, S. I., Lehsten, V., Reick, C. H., Rietkerk, M., Scheiter, S., Yin, Z.,
605 Zavala, M. A., and Brovkin, V.: Forests, savannas, and grasslands: bridging the knowledge gap between ecology and Dynamic Global Vegetation Models, *Biogeosciences*, 12, 1833–1848, <https://doi.org/10.5194/bg-12-1833-2015>, <https://www.biogeosciences.net/12/1833/2015/>, 2015.
- Beck, H. E., Zimmermann, N. E., McVicar, T. R., Vergopolan, N., Berg, A., and Wood, E. F.: Present and future Köppen-Geiger climate classification maps at 1-km resolution, *Scientific Data*, 5, 180214, <https://doi.org/10.1038/sdata.2018.214>, <https://www.nature.com/articles/sdata2018214>, number: 1 Publisher: Nature Publishing Group, 2018.
- 610 Beerling, D. J. and Osborne, C. P.: The origin of the savanna biome, *Global Change Biology*, 12, 2023–2031, <https://doi.org/https://doi.org/10.1111/j.1365-2486.2006.01239.x>, <http://onlinelibrary.wiley.com/doi/abs/10.1111/j.1365-2486.2006.01239.x>, [_eprint: https://onlinelibrary.wiley.com/doi/pdf/10.1111/j.1365-2486.2006.01239.x](https://onlinelibrary.wiley.com/doi/pdf/10.1111/j.1365-2486.2006.01239.x), 2006.
- Beringer, J., Hutley, L. B., McHugh, I., Arndt, S. K., Campbell, D., Cleugh, H. A., Cleverly, J., Resco de Dios, V., Eamus, D., Evans,
615 B., Ewenz, C., Grace, P., Griebel, A., Haverd, V., Hinko-Najera, N., Huete, A., Isaac, P., Kanniah, K., Leuning, R., Liddell, M. J., Macfarlane, C., Meyer, W., Moore, C., Pendall, E., Phillips, A., Phillips, R. L., Prober, S. M., Restrepo-Coupe, N., Rutledge, S., Schroder, I., Silberstein, R., Southall, P., Yee, M. S., Tapper, N. J., van Gorsel, E., Vote, C., Walker, J., and Wardlaw, T.: An introduction to the Australian and New Zealand flux tower network –OzFlux, *Biogeosciences*, 13, 5895–5916, <https://doi.org/10.5194/bg-13-5895-2016>, <https://www.biogeosciences.net/13/5895/2016/>, 2016.
- 620 Beringer, J., McHugh, I., Hutley, L. B., Isaac, P., and Kljun, N.: Technical note: Dynamic INtegrated Gap-filling and partitioning for OzFlux (DINGO), *Biogeosciences*, 14, 1457–1460, <https://doi.org/10.5194/bg-14-1457-2017>, <https://www.biogeosciences.net/14/1457/2017/>, 2017.
- Best, M. J., Abramowitz, G., Johnson, H. R., Pitman, A. J., Balsamo, G., Boone, A., Cuntz, M., Decharme, B., Dirmeyer, P. A., Dong, J., Ek, M., Guo, Z., Haverd, V., van den Hurk, B. J. J., Nearing, G. S., Pak, B., Peters-Lidard, C., Santanello, J. A., Stevens, L., and
625 Vuichard, N.: The Plumbing of Land Surface Models: Benchmarking Model Performance, *Journal of Hydrometeorology*, 16, 1425–1442, <https://doi.org/10.1175/JHM-D-14-0158.1>, <http://journals.ametsoc.org/doi/10.1175/JHM-D-14-0158.1>, 2015.
- Bierkens, M. F. P. and van den Hurk, B. J. J. M.: Groundwater convergence as a possible mechanism for multi-year persistence in rainfall, *Geophysical Research Letters*, 34, <https://doi.org/10.1029/2006GL028396>, <http://agupubs.onlinelibrary.wiley.com/doi/abs/10.1029/2006GL028396>, 2007.
- 630 Bonan, G. B., Williams, M., Fisher, R. A., and Oleson, K. W.: Modeling stomatal conductance in the earth system: linking leaf water-use efficiency and water transport along the soil–plant–atmosphere continuum, *Geosci. Model Dev.*, 7, 2193–2222, <https://doi.org/10.5194/gmd-7-2193-2014>, <http://www.geosci-model-dev.net/7/2193/2014/>, 2014.



- Buckley, T. N., Sack, L., and Farquhar, G. D.: Optimal plant water economy, *Plant, Cell & Environment*, 40, 881–896, <https://doi.org/10.1111/pce.12823>, <http://doi.wiley.com/10.1111/pce.12823>, 2017.
- 635 Carsel, R. F. and Parrish, R. S.: Developing joint probability distributions of soil water retention characteristics, *Water Resources Research*, 24, 755–769, <https://doi.org/10.1029/WR024i005p00755>, <http://agupubs.onlinelibrary.wiley.com/doi/abs/10.1029/WR024i005p00755>,
_eprint: <https://onlinelibrary.wiley.com/doi/pdf/10.1029/WR024i005p00755>, 1988.
- Choudhury, B. J.: Relationships between vegetation indices, radiation absorption, and net photosynthesis evaluated by a sensitivity analysis, *Remote Sensing of Environment*, 22, 209–233, [https://doi.org/10.1016/0034-4257\(87\)90059-9](https://doi.org/10.1016/0034-4257(87)90059-9), <https://linkinghub.elsevier.com/retrieve/pii/0034425787900599>, 1987.
- 640 De Kauwe, M. G., Kala, J., Lin, Y.-S., Pitman, A. J., Medlyn, B. E., Duursma, R. A., Abramowitz, G., Wang, Y.-P., and Miralles, D. G.: A test of an optimal stomatal conductance scheme within the CABLE land surface model, *Geoscientific Model Development*, 8, 431–452, <https://doi.org/10.5194/gmd-8-431-2015>, <http://www.geosci-model-dev.net/8/431/2015/>, 2015.
- Dekker, S. C., Vrugt, J. A., and Elkington, R. J.: Significant variation in vegetation characteristics and dynamics from ecohydrological optimality of net carbon profit, *Ecohydrology*, 5, 1–18, <https://doi.org/10.1002/eco.177>, <http://onlinelibrary.wiley.com/doi/abs/10.1002/eco.177>, 2010.
- Dirmeyer, P. A.: A History and Review of the Global Soil Wetness Project (GSWP), *Journal of Hydrometeorology*, 12, 729–749, <https://doi.org/10.1175/JHM-D-10-05010.1>, <https://journals.ametsoc.org/jhm/article/12/5/729/5747/A-History-and-Review-of-the-Global-Soil-Wetness>, 2011.
- 650 Donohue, R., McVicar, T., and Roderick, M.: Australian monthly fPAR derived from Advanced Very High Resolution Radiometer reflectances - version 5. v1. CSIRO. Data Collection., <https://doi.org/10.4225/08/50FE0CBE0DD06>, 2013.
- Donohue, R. J., Roderick, M. L., and McVicar, T. R.: Deriving consistent long-term vegetation information from AVHRR reflectance data using a cover-triangle-based framework, *Remote Sensing of Environment*, 112, 2938–2949, <https://doi.org/10.1016/j.rse.2008.02.008>, <http://linkinghub.elsevier.com/retrieve/pii/S0034425708000618>, 2008.
- 655 Duan, Q., Sorooshian, S., and Gupta, V. K.: Optimal use of the SCE-UA global optimization method for calibrating watershed models, *Journal of Hydrology*, 158, 265–284, [https://doi.org/10.1016/0022-1694\(94\)90057-4](https://doi.org/10.1016/0022-1694(94)90057-4), <http://www.sciencedirect.com/science/article/pii/0022169494900574>, 1994.
- Duursma, R. A. and Medlyn, B. E.: MAESPA: a model to study interactions between water limitation, environmental drivers and vegetation function at tree and stand levels, with an example application to [CO₂] × drought interactions, *Geoscientific Model Development*, 5, 919–940, <https://doi.org/10.5194/gmd-5-919-2012>, <https://www.geosci-model-dev.net/5/919/2012/>, 2012.
- 660 Eagleson, P. S.: Ecological optimality in water-limited natural soil-vegetation systems: 1. Theory and hypothesis, *Water Resources Research*, 18, 325–340, <https://doi.org/10.1029/WR018i002p00325>, <http://agupubs.onlinelibrary.wiley.com/doi/abs/10.1029/WR018i002p00325>, 1982.
- Eamus, D., O’Grady, A., and Hutley, L.: Dry season conditions determine wet season water use in the wet-tropical savannas of northern Australia, *Tree physiology*, 20, 1219–1226, <https://doi.org/10.1093/treephys/20.18.1219>, 2000.
- Faticchi, S., Ivanov, V. Y., and Caporali, E.: A mechanistic ecohydrological model to investigate complex interactions in cold and warm water-controlled environments: 1. Theoretical framework and plot-scale analysis, *Journal of Advances in Modeling Earth Systems*, 4, <https://doi.org/10.1029/2011MS000086>, <https://agupubs.onlinelibrary.wiley.com/doi/abs/10.1029/2011MS000086>, 2012.



- Franklin, O., Johansson, J., Dewar, R. C., Dieckmann, U., McMurtrie, R. E., Brännström, A., and Dybzinski, R.: Modeling carbon allocation
670 in trees: a search for principles, *Tree Physiology*, <https://doi.org/10.1093/treephys/tpr138>, <http://treephys.oxfordjournals.org/content/early/2012/02/15/treephys.tpr138>, 2012.
- Franklin, O., Harrison, S. P., Dewar, R., Farrior, C. E., Brännström, A., Dieckmann, U., Pietsch, S., Falster, D., Cramer, W., Loreau, M.,
Wang, H., Mäkelä, A., Rebel, K. T., Meron, E., Schymanski, S. J., Rovenskaya, E., Stocker, B. D., Zaehle, S., Manzoni, S., van Oijen,
M., Wright, I. J., Ciais, P., van Bodegom, P. M., Peñuelas, J., Hofhansl, F., Terrer, C., Soudzilovskaia, N. A., Midgley, G., and Prentice,
675 I. C.: Organizing principles for vegetation dynamics, *Nature Plants*, 6, 444–453, <https://doi.org/10.1038/s41477-020-0655-x>, <https://www.nature.com/articles/s41477-020-0655-x>, number: 5 Publisher: Nature Publishing Group, 2020.
- Grace, J., José, J. S., Meir, P., Miranda, H. S., and Montes, R. A.: Productivity and carbon fluxes of tropical savannas, *Journal of Biogeog-*
raphy, 33, 387–400, <https://doi.org/10.1111/j.1365-2699.2005.01448.x>, <http://onlinelibrary.wiley.com/doi/abs/10.1111/j.1365-2699.2005.01448.x>, 2006.
- 680 Hacke, U. G., Sperry, J. S., Pockman, W. T., Davis, S. D., and McCulloh, K. A.: Trends in wood density and structure are linked to preven-
tion of xylem implosion by negative pressure, *Oecologia*, 126, 457–461, <https://doi.org/10.1007/s004420100628>, <https://doi.org/10.1007/s004420100628>, 2001.
- Haverd, V., Raupach, M. R., Briggs, P. R., Canadell, J. G., Isaac, P., Pickett-Heaps, C., Roxburgh, S. H., van Gorsel, E., Viscarra Rossel,
R. A., and Wang, Z.: Multiple observation types reduce uncertainty in Australia’s terrestrial carbon and water cycles, *Biogeosciences*, 10,
685 2011–2040, <https://doi.org/10.5194/bg-10-2011-2013>, <https://www.biogeosciences.net/10/2011/2013/>, 2013.
- Haverd, V., Smith, B., Raupach, M., Briggs, P., Nieradzick, L., Beringer, J., Hutley, L., Trudinger, C. M., and Cleverly, J.: Coupling carbon
allocation with leaf and root phenology predicts tree–grass partitioning along a savanna rainfall gradient, *Biogeosciences*, 13, 761–779,
<https://doi.org/10.5194/bg-13-761-2016>, <http://www.biogeosciences.net/13/761/2016/>, 2016.
- House, J. I., Archer, S., Breshears, D. D., and Scholes, R. J.: Conundrums in mixed woody–herbaceous plant systems, *Journal of Biogeog-*
raphy, 30, 1763–1777, <https://doi.org/https://doi.org/10.1046/j.1365-2699.2003.00873.x>, [http://onlinelibrary.wiley.com/doi/abs/10.1046/](http://onlinelibrary.wiley.com/doi/abs/10.1046/j.1365-2699.2003.00873.x)
690 [j.1365-2699.2003.00873.x](http://onlinelibrary.wiley.com/doi/pdf/10.1046/j.1365-2699.2003.00873.x), _eprint: <https://onlinelibrary.wiley.com/doi/pdf/10.1046/j.1365-2699.2003.00873.x>, 2003.
- Hutley, L. B.: Vegetation Above Ground Biomass, Litchfield Savanna SuperSite, Tower Plot, 2013, <https://supersites.tern.org.au/knb/metacat/supersite.118.6/html>, 2015.
- Hutley, L. B., O’Grady, A. P., and Eamus, D.: Evapotranspiration from Eucalypt open-forest savanna of Northern Australia, *Functional*
Ecology, 14, 183–194, <https://doi.org/https://doi.org/10.1046/j.1365-2435.2000.00416.x>, <https://besjournals.onlinelibrary.wiley.com/doi/abs/10.1046/j.1365-2435.2000.00416.x>,
695 [_eprint: https://besjournals.onlinelibrary.wiley.com/doi/pdf/10.1046/j.1365-2435.2000.00416.x](https://besjournals.onlinelibrary.wiley.com/doi/pdf/10.1046/j.1365-2435.2000.00416.x), 2000.
- Hutley, L. B., Beringer, J., Isaac, P. R., Hacker, J. M., and Cernusak, L. A.: A sub-continental scale living laboratory: Spatial pat-
terns of savanna vegetation over a rainfall gradient in northern Australia, *Agricultural and Forest Meteorology*, 151, 1417–1428,
700 <https://doi.org/10.1016/j.agrformet.2011.03.002>, <http://www.sciencedirect.com/science/article/pii/S0168192311000839>, 2011.
- Jeffrey, S. J., Carter, J. O., Moodie, K. B., and Beswick, A. R.: Using spatial interpolation to construct a comprehensive archive of Australian
climate data, *Environmental Modelling & Software*, 16, 309–330, [https://doi.org/10.1016/S1364-8152\(01\)00008-1](https://doi.org/10.1016/S1364-8152(01)00008-1), <https://linkinghub.elsevier.com/retrieve/pii/S1364815201000081>, 2001.
- Keeling, C. D., Piper, S. C., Bacastow, R. B., Wahlen, M., Whorf, T. P., Heimann, M., and Meijer, H. A.: Atmospheric CO₂ and 13CO₂
705 Exchange with the Terrestrial Biosphere and Oceans from 1978 to 2000: Observations and Carbon Cycle Implications, in: *A History of*



- Atmospheric CO₂ and its effects on Plants, Animals, and Ecosystems, pp. 83–113, Springer Verlag, New York, editors: Ehleringer, J.R., T. E. Cerling, M. D. Dearing, 2005.
- 710 Kelley, G., O’Grady, A. P., Hutley, L. B., and Eamus, D.: A comparison of tree water use in two contiguous vegetation communities of the seasonally dry tropics of northern Australia: the importance of site water budget to tree hydraulics, *Australian Journal of Botany*, 55, 700–708, <https://doi.org/10.1071/BT07021>, <https://www.publish.csiro.au/bt/BT07021>, 2007.
- Kollet, S. J. and Maxwell, R. M.: Capturing the influence of groundwater dynamics on land surface processes using an integrated, distributed watershed model, *Water Resources Research*, 44, <https://doi.org/10.1029/2007WR006004>, <https://agupubs.onlinelibrary.wiley.com/doi/abs/10.1029/2007WR006004>, 2008.
- 715 Kowalczyk, E. A., Wang, Y. P., Law, R. M., Davies, H. L., McGregor, J. L., and Abramowitz, G.: The CSIRO Atmosphere Biosphere Land Exchange (CABLE) model for use in climate models and as an offline model, *Tech. rep.*, CSIRO, 2006.
- Lehmann, C. E. R., Anderson, T. M., Sankaran, M., Higgins, S. I., Archibald, S., Hoffmann, W. A., Hanan, N. P., Williams, R. J., Fensham, R. J., Felfili, J., Hutley, L. B., Ratnam, J., Jose, J. S., Montes, R., Franklin, D., Russell-Smith, J., Ryan, C. M., Durigan, G., Hiernaux, P., Haidar, R., Bowman, D. M. J. S., and Bond, W. J.: Savanna Vegetation-Fire-Climate Relationships Differ Among Continents, *Science*, 343, 548–552, <https://doi.org/10.1126/science.1247355>, <http://science.sciencemag.org/content/343/6170/548>, 2014.
- 720 Lu, H.: Decomposition of vegetation cover into woody and herbaceous components using AVHRR NDVI time series, *Remote Sensing of Environment*, 86, 1–18, [https://doi.org/10.1016/S0034-4257\(03\)00054-3](https://doi.org/10.1016/S0034-4257(03)00054-3), <https://linkinghub.elsevier.com/retrieve/pii/S0034425703000543>, 2003.
- Ma, X., Huete, A., Yu, Q., Coupe, N. R., Davies, K., Broich, M., Ratana, P., Beringer, J., Hutley, L. B., Cleverly, J., Boulain, N., and Eamus, D.: Spatial patterns and temporal dynamics in savanna vegetation phenology across the North Australian Tropical Transect, *Remote Sensing of Environment*, 139, 97–115, <https://doi.org/10.1016/j.rse.2013.07.030>, <https://linkinghub.elsevier.com/retrieve/pii/S0034425713002423>, 2013.
- 725 Maxwell, R. M., Chow, F. K., and Kollet, S. J.: The groundwater–land-surface–atmosphere connection: Soil moisture effects on the atmospheric boundary layer in fully-coupled simulations, *Advances in Water Resources*, 30, 2447–2466, <https://doi.org/10.1016/j.advwatres.2007.05.018>, <https://linkinghub.elsevier.com/retrieve/pii/S0309170807000954>, 2007.
- 730 McDonnell, J. J., Sivapalan, M., Vaché, K., Dunn, S., Grant, G., Haggerty, R., Hinz, C., Hooper, R., Kirchner, J., Roderick, M. L., Selker, J., and Weiler, M.: Moving beyond heterogeneity and process complexity: A new vision for watershed hydrology, *Water Resources Research*, 43, <https://doi.org/10.1029/2006WR005467>, <https://agupubs.onlinelibrary.wiley.com/doi/abs/10.1029/2006WR005467>, 2007.
- 735 Mencuccini, M., Hölttä, T., Petit, G., and Magnani, F.: Sanio’s laws revisited. Size-dependent changes in the xylem architecture of trees, *Ecology Letters*, 10, 1084–1093, <https://doi.org/10.1111/j.1461-0248.2007.01104.x>, <http://onlinelibrary.wiley.com/doi/abs/10.1111/j.1461-0248.2007.01104.x>, 2007.
- Moore, C. E., Beringer, J., Evans, B., Hutley, L. B., McHugh, I., and Tapper, N. J.: The contribution of trees and grasses to productivity of an Australian tropical savanna, *Biogeosciences*, 13, 2387–2403, <https://doi.org/10.5194/bg-13-2387-2016>, <https://bg.copernicus.org/articles/13/2387/2016/>, 2016.
- 740 Nijzink, R. C., Beringer, J., Hutley, L. B., and Schymanski, S. J.: Technical note: Updates and modifications to the Vegetation Optimality Model for comparability, In preparation, 2021.
- O’Grady, A. P., Eamus, D., and Hutley, L. B.: Transpiration increases during the dry season: patterns of tree water use in eucalypt open-forests of northern Australia, *Tree Physiology*, 19, 591–597, <https://doi.org/10.1093/treephys/19.9.591>, 1999.



- Peel, M. C., Finlayson, B. L., and McMahon, T. A.: Updated world map of the Köppen-Geiger climate classification, *Hydrol. Earth Syst. Sci.*, p. 12, 2007.
- 745 Pitman, A. J., Henderson-Sellers, A., Desborough, C. E., Yang, Z.-L., Abramopoulos, F., Boone, A., Dickinson, R. E., Gedney, N., Koster, R., Kowalczyk, E., Lettenmaier, D., Liang, X., Mahfouf, J.-F., Noilhan, J., Polcher, J., Qu, W., Rocco, A., Rosenzweig, C., Schlosser, C. A., Shmakin, A. B., Smith, J., Suarez, M., Verseghy, D., Wetzel, P., Wood, E., and Xue, Y.: Key results and implications from phase 1(c) of the Project for Intercomparison of Land-surface Parametrization Schemes, *Climate Dynamics*, 15, 673–684, <https://doi.org/10.1007/s003820050309>, <http://link.springer.com/10.1007/s003820050309>, 1999.
- 750 Pitman, A. J., Noblet-Ducoudré, N. d., Cruz, F. T., Davin, E. L., Bonan, G. B., Brovkin, V., Claussen, M., Delire, C., Ganzeveld, L., Gayler, V., Hurk, B. J. J. M. v. d., Lawrence, P. J., Molen, M. K. v. d., Müller, C., Reick, C. H., Seneviratne, S. I., Strengers, B. J., and Voldoire, A.: Uncertainties in climate responses to past land cover change: First results from the LUCID intercomparison study, *Geophysical Research Letters*, 36, <https://doi.org/https://doi.org/10.1029/2009GL039076>, <http://agupubs.onlinelibrary.wiley.com/doi/abs/10.1029/2009GL039076>, _eprint: <https://onlinelibrary.wiley.com/doi/pdf/10.1029/2009GL039076>, 2009.
- 755 Prentice, I. C., Liang, X., Medlyn, B. E., and Wang, Y.-P.: Reliable, robust and realistic: the three R's of next-generation land-surface modelling, *Atmos. Chem. Phys.*, 15, 5987–6005, <https://doi.org/10.5194/acp-15-5987-2015>, <https://www.atmos-chem-phys.net/15/5987/2015/>, 2015.
- Roderick, M. L. and Berry, S. L.: Linking wood density with tree growth and environment: a theoretical analysis based on the motion of water, *New Phytologist*, 149, 473–485, 2001.
- 760 Rodríguez-Iturbe, I. and Rinaldo, A.: *Fractal River Basins: Chance and Self-Organization*, Cambridge University Press, google-Books-ID: _xjhtl7zeB8C, 2001.
- Rowe, C., Wurster, C. M., Zwart, C., Brand, M., Hutley, L. B., Levchenko, V., and Bird, M. I.: Vegetation over the last glacial maximum at Girraween Lagoon, monsoonal northern Australia, *Quaternary Research*, pp. 1–14, <https://doi.org/10.1017/qua.2020.50>, <https://www.cambridge.org/core/journals/quaternary-research/article/abs/vegetation-over-the-last-glacial-maximum-at-girraween-lagoon-monsoonal-northern-australia/5F65879E0F1ADA256F1A7341A7B4F5F1>, publisher: Cambridge University Press, 2020.
- 765 quaternary-research/article/abs/vegetation-over-the-last-glacial-maximum-at-girraween-lagoon-monsoonal-northern-australia/5F65879E0F1ADA256F1A7341A7B4F5F1, publisher: Cambridge University Press, 2020.
- Ryu, Y., Baldocchi, D. D., Kobayashi, H., Ingen, C. v., Li, J., Black, T. A., Beringer, J., Gorsel, E. v., Knohl, A., Law, B. E., and Rouspard, O.: Integration of MODIS land and atmosphere products with a coupled-process model to estimate gross primary productivity and evapotranspiration from 1 km to global scales, *Global Biogeochemical Cycles*, 25, <https://doi.org/10.1029/2011GB004053>, <https://agupubs.onlinelibrary-wiley-com.proxy.bnl.lu/doi/10.1029/2011GB004053>, 2011.
- 770 <https://agupubs.onlinelibrary-wiley-com.proxy.bnl.lu/doi/10.1029/2011GB004053>, 2011.
- Ryu, Y., Baldocchi, D. D., Black, T. A., Detto, M., Law, B. E., Leuning, R., Miyata, A., Reichstein, M., Vargas, R., Ammann, C., Beringer, J., Flanagan, L. B., Gu, L., Hutley, L. B., Kim, J., McCaughey, H., Moors, E. J., Rambal, S., and Vesala, T.: On the temporal upscaling of evapotranspiration from instantaneous remote sensing measurements to 8-day mean daily-sums, *Agricultural and Forest Meteorology*, 152, 212–222, <https://doi.org/10.1016/j.agrformet.2011.09.010>, <https://linkinghub.elsevier.com/retrieve/pii/S0168192311002863>, 2012.
- 775 Savenije, H. H. G.: The importance of interception and why we should delete the term evapotranspiration from our vocabulary, *Hydrological Processes*, 18, 1507–1511, <https://doi.org/10.1002/hyp.5563>, <http://onlinelibrary.wiley.com/doi/abs/10.1002/hyp.5563>, _eprint: <https://onlinelibrary.wiley.com/doi/pdf/10.1002/hyp.5563>, 2004.
- Scheiter, S. and Higgins, S. I.: Impacts of climate change on the vegetation of Africa: an adaptive dynamic vegetation modelling approach, *Global Change Biology*, 15, 2224–2246, <https://doi.org/10.1111/j.1365-2486.2008.01838.x>, <http://onlinelibrary.wiley.com/doi/abs/10.1111/j.1365-2486.2008.01838.x>, _eprint: <https://onlinelibrary.wiley.com/doi/pdf/10.1111/j.1365-2486.2008.01838.x>, 2009.
- 780 <https://onlinelibrary.wiley.com/doi/pdf/10.1111/j.1365-2486.2008.01838.x>, 2009.



- Scheiter, S., Langan, L., and Higgins, S. I.: Next-generation dynamic global vegetation models: learning from community ecology, *New Phytologist*, 198, 957–969, <https://doi.org/10.1111/nph.12210>, <https://nph.onlinelibrary.wiley.com/doi/abs/10.1111/nph.12210>, <https://nph.onlinelibrary.wiley.com/doi/pdf/10.1111/nph.12210>, 2013.
- Scheiter, S., Higgins, S. I., Beringer, J., and Hutley, L. B.: Climate change and long-term fire management impacts on Australian savannas, *New Phytologist*, 205, 1211–1226, <https://doi.org/10.1111/nph.13130>, <https://nph.onlinelibrary.wiley.com/doi/abs/10.1111/nph.13130>, [_eprint: https://nph.onlinelibrary.wiley.com/doi/pdf/10.1111/nph.13130](https://nph.onlinelibrary.wiley.com/doi/pdf/10.1111/nph.13130), 2015.
- Schenk, H. J. and Jackson, R. B.: Rooting depths, lateral root spreads and below-ground/above-ground allometries of plants in water-limited ecosystems, *Journal of Ecology*, 90, 480–494, 2002.
- Scholes, R. J. and Archer, S. R.: Tree-Grass Interactions in Savannas, *Annual Review of Ecology and Systematics*, 28, 517–544, <https://doi.org/10.1146/annurev.ecolsys.28.1.517>, <https://doi.org/10.1146/annurev.ecolsys.28.1.517>, [_eprint: https://doi.org/10.1146/annurev.ecolsys.28.1.517](https://doi.org/10.1146/annurev.ecolsys.28.1.517), 1997.
- Schulz, K., Jarvis, A., Beven, K., and Soegaard, H.: The predictive uncertainty of land surface fluxes in response to increasing ambient carbon dioxide, *Journal of Climate*, 14, 2551–2562, 2001.
- Schymanski, S. J., Roderick, M. L., Sivapalan, M., Hutley, L. B., and Beringer, J.: A test of the optimality approach to modelling canopy properties and CO₂ uptake by natural vegetation, *Plant, Cell & Environment*, 30, 1586–1598, <https://doi.org/10.1111/j.1365-3040.2007.01728.x>, <http://www.blackwell-synergy.com/doi/abs/10.1111/j.1365-3040.2007.01728.x>, 2007.
- Schymanski, S. J., Sivapalan, M., Roderick, M. L., Beringer, J., and Hutley, L. B.: An optimality-based model of the coupled soil moisture and root dynamics, *Hydrology and Earth System Sciences*, 12, 913–932, <https://doi.org/10.5194/hess-12-913-2008>, <http://www.hydrol-earth-syst-sci.net/12/913/2008/>, 2008.
- Schymanski, S. J., Kleidon, A., and Roderick, M. L.: Ecohydrological Optimality, in: *Encyclopedia of Hydrological Sciences*, American Cancer Society, <https://doi.org/10.1002/0470848944.hsa319>, <https://onlinelibrary.wiley.com/doi/abs/10.1002/0470848944.hsa319>, 2009a.
- Schymanski, S. J., Sivapalan, M., Roderick, M. L., Hutley, L. B., and Beringer, J.: An optimality-based model of the dynamic feedbacks between natural vegetation and the water balance, *Water Resources Research*, 45, <https://doi.org/10.1029/2008WR006841>, <https://agupubs.onlinelibrary-wiley-com.proxy.bnl.lu/doi/full/10.1029/2008WR006841>, 2009b.
- Schymanski, S. J., Roderick, M. L., and Sivapalan, M.: Using an optimality model to understand medium and long-term responses of vegetation water use to elevated atmospheric CO₂ concentrations, *AoB Plants*, 7, plv060, <https://doi.org/10.1093/aobpla/plv060>, <http://aobpla.oxfordjournals.org/content/7/plv060>, 2015.
- Smith, B., Prentice, I. C., and Sykes, M. T.: Representation of vegetation dynamics in the modelling of terrestrial ecosystems: comparing two contrasting approaches within European climate space, *Global Ecology and Biogeography*, 10, 621–637, <https://doi.org/10.1046/j.1466-822X.2001.t01-1-00256.x>, <http://onlinelibrary.wiley.com/doi/abs/10.1046/j.1466-822X.2001.t01-1-00256.x>, 2001.
- Tague, C. L.: RHESSys: Regional Hydro-Ecologic Simulation System—An Object- Oriented Approach to Spatially Distributed Modeling of Carbon, Water, and Nutrient Cycling, *Earth Interactions*, p. 42, 2004.
- Teckentrup, L., De Kauwe, M. G., Pitman, A. J., Goll, D., Haverd, V., Jain, A. K., Joetzjer, E., Kato, E., Lienert, S., Lombardozzi, D., McGuire, P. C., Melton, J. R., Nabel, J. E. M. S., Pongratz, J., Sitch, S., Walker, A. P., and Zaehle, S.: Assessing the representation of the Australian carbon cycle in global vegetation models, *Biogeosciences Discussions*, pp. 1–47, <https://doi.org/10.5194/bg-2021-66>, <https://bg.copernicus.org/preprints/bg-2021-66/>, publisher: Copernicus GmbH, 2021.
- Van Genuchten, M. T.: A Closed-form Equation for Predicting the Hydraulic Conductivity of Unsaturated Soils, *Soil Science Society of America Journal*, 44, 892–898, <https://doi.org/https://doi.org/10.2136/sssaj1980.03615995004400050002x>, <http://access.onlinelibrary>.



- wiley.com/doi/abs/10.2136/sssaj1980.03615995004400050002x, _eprint: https://onlinelibrary.wiley.com/doi/pdf/10.2136/sssaj1980.03615995004400050002x,
820 1980.
- Viscarra Rossel, R., Chen, C., Grundy, M., Searle, R., Clifford, D., Odgers, N., Holmes, K., Griffin, T., Liddicoat, C., and Kidd, D.: Soil and Landscape Grid National Soil Attribute Maps - Clay (3" resolution) - Release 1, <https://doi.org/10.4225/08/546EEE35164BF>, <https://data.csiro.au/collections/#collection/CIcsiro:10168v5>, type: dataset, 2014a.
- Viscarra Rossel, R., Chen, C., Grundy, M., Searle, R., Clifford, D., Odgers, N., Holmes, K., Griffin, T., Liddicoat, C., and Kidd, D.: Soil
825 and Landscape Grid National Soil Attribute Maps - Silt (3" resolution) - Release 1, <https://doi.org/10.4225/08/546F48D6A6D48>, <https://data.csiro.au/collections/#collection/CIcsiro:10688v5>, type: dataset, 2014b.
- Viscarra Rossel, R., Chen, C., Grundy, M., Searle, R., Clifford, D., Odgers, N., Holmes, K., Griffin, T., Liddicoat, C., and Kidd, D.: Soil and Landscape Grid National Soil Attribute Maps - Sand (3" resolution) - Release 1, <https://doi.org/10.4225/08/546F29646877E>, <https://data.csiro.au/collections/#collection/CIcsiro:10149v5>, type: dataset, 2014c.
- 830 Wang, H., Prentice, I. C., Keenan, T. F., Davis, T. W., Wright, I. J., Cornwell, W. K., Evans, B. J., and Peng, C.: Towards a universal model for carbon dioxide uptake by plants, *Nature Plants*, 3, 734–741, <https://doi.org/10.1038/s41477-017-0006-8>, <http://www.nature.com/articles/s41477-017-0006-8>, 2017.
- Wang, P., Niu, G., Fang, Y., Wu, R., Yu, J., Yuan, G., Pozdniakov, S. P., and Scott, R. L.: Implementing Dynamic Root Optimization in Noah-MP for Simulating Phreatophytic Root Water Uptake, *Water Resources Research*, 54, 1560–1575,
835 <https://doi.org/10.1002/2017WR021061>, <https://onlinelibrary.wiley.com/doi/abs/10.1002/2017WR021061>, 2018.
- Wang, Y. P., Kowalczyk, E., Leuning, R., Abramowitz, G., Raupach, M. R., Pak, B., Gorsel, E. v., and Luhar, A.: Diagnosing errors in a land surface model (CABLE) in the time and frequency domains, *Journal of Geophysical Research: Biogeosciences*, 116, <https://doi.org/10.1029/2010JG001385>, <https://agupubs.onlinelibrary.wiley.com/doi/abs/10.1029/2010JG001385>, 2011.
- Whitley, R., Beringer, J., Hutley, L. B., Abramowitz, G., De Kauwe, M. G., Duursma, R., Evans, B., Haverd, V., Li, L., Ryu, Y., Smith,
840 B., Wang, Y.-P., Williams, M., and Yu, Q.: A model inter-comparison study to examine limiting factors in modelling Australian tropical savannas, *Biogeosciences*, 13, 3245–3265, <https://doi.org/10.5194/bg-13-3245-2016>, <http://www.biogeosciences.net/13/3245/2016/>, 2016.
- Williams, M., Rastetter, E. B., Fernandes, D. N., Goulden, M. L., Wofsy, S. C., Shaver, G. R., Melillo, J. M., Munger, J. W., Fan, S.-M., and Nadelhoffer, K. J.: Modelling the soil-plant-atmosphere continuum in a Quercus–Acer stand at Harvard Forest: the regulation of stomatal conductance by light, nitrogen and soil/plant hydraulic properties, *Plant, Cell & Environment*, 19, 911–927, <https://doi.org/10.1111/j.1365-3040.1996.tb00456.x>, <http://onlinelibrary.wiley.com/doi/abs/10.1111/j.1365-3040.1996.tb00456.x>, 1996a.
- Williams, R. J., Duff, G. A., Bowman, D. M. J. S., and Cook, G. D.: Variation in the composition and structure of tropical savannas as a function of rainfall and soil texture along a large-scale climatic gradient in the Northern Territory, Australia, *Journal of Biogeography*, 23, 747–756, <https://doi.org/10.1111/j.1365-2699.1996.tb00036.x>, <https://onlinelibrary.wiley.com/doi/abs/10.1111/j.1365-2699.1996.tb00036.x>, 1996b.
850
- York, J. P., Person, M., Gutowski, W. J., and Winter, T. C.: Putting aquifers into atmospheric simulation models: an example from the Mill Creek Watershed, northeastern Kansas, *Advances in Water Resources*, 25, 221–238, [https://doi.org/10.1016/S0309-1708\(01\)00021-5](https://doi.org/10.1016/S0309-1708(01)00021-5), <https://linkinghub.elsevier.com/retrieve/pii/S0309170801000215>, 2002.